arXiv:2202.06009v2 [cs.LG] 13 Mar 2022

Maximizing Communication Efficiency for Large-scale Training via 0/1 Adam

Yucheng Lu [1] **Conglong Li** [2] **Minjia Zhang** [2] **Christopher De Sa** [1] **Yuxiong He** [2]

Abstract

1-bit communication is an effective method to scale up model training, and has been studied extensively on SGD. Its benefits, however, remain an open question on Adam-based model training (e.g. BERT and GPT). In this paper, we propose **0/1 Adam**, which improves upon the state-of-the-art 1-bit Adam via two novel designs: (1) *adaptive variance state freezing*, which eliminates the requirement of running expensive full-precision communication at early stage of training; (2) *1-bit sync*, which allows skipping communication rounds with bit-free synchronization over Adam's optimizer states, momentum and variance. In theory, we provide convergence analysis for **0/1 Adam** on smooth non-convex objectives, and show the complexity bound is better than original Adam under certain conditions. On various benchmarks such as BERT-Base/Large pretraining and ImageNet, we demonstrate on up to 128 GPUs that **0/1 Adam** is able to reduce up to 87% of data volume, 54% of communication rounds, and achieve up to 2× higher throughput compared to the state-of-the-art 1-bit Adam while enjoying the same statistical convergence speed and end-to-end model accuracy on GLUE dataset and ImageNet validation set.

1. Introduction

When training large models (such as BERT and GPT-2) on commodity systems with limited bandwidth, the communication overhead across computing nodes is a crucial bottleneck that hinders scalability. 1-bit communication is an effective method to mitigate this problem by aggressively quantizing all the communicated tensors using their signs with a shared magnitude across coordinates (Seide et al., 2014; Bernstein et al., 2018a). While 1-bit communication demonstrates tremendous success on distributed SGD, its benefits over large-scale Adam-based model training, such as for BERT and GPT pretraining, remains an open question (Kingma & Ba, 2014; Wang et al., 2019a).

Limitations of the state-of-the-art 1-bit Adam. Tang et al. (2021) undertook the first investigation of this question and proposed **1-bit Adam**. The algorithm follows a two-stage training paradigm: first run Adam with full-precision communication (*full-precision stage*[1]); and then switch to 1 bit when the variance state, i.e. the running average of second moment gradient in Adam, becomes stable (*compression stage*). While this paradigm allows drastic data volume reduction over original Adam, the experimental results from (Tang et al., 2021) indicate the full-precision stage still incurs non-trivial overhead. For instance, it is shown that when training the BERT-Large model, 1-bit Adam sends each parameter with 3.27 bits on average, which is not close to 1 bit as we would expect. Furthermore, our study in Section 3 reveals that since large models like BERT and GPT are trained with Adam on a large number of GPUs, even during compression stage, the fixed cost of initiating 1-bit communication and compression can still become a bottleneck that limits the end-to-end throughput gain.

Challenges on improving 1-bit Adam. In correspondence to the limitations of 1-bit Adam, one natural idea is to remove the full-precision stage, and then potentially skip some 1-bit communication rounds. This overall motivation seems well-aligned with the classic works on 1-bit SGD (Bernstein et al., 2018a) and local SGD (Stich, 2018). However, this natural idea cannot be applied to Adam directly due to two main challenges: (1) (1-bit) Adam has additional optimizer states, momentum and variance, that are sensitive to compression at early stage of training. The naive removal of full-precision stage could easily cause slow convergence or even divergence. (2) While local SGD guarantees all the workers can optimize the same model parameters via periodic model synchronization, (1-bit) Adam requires additional synchronization over momentum and variance, which otherwise would fail to capture the global gradient moments dynamics on each worker locally. This additional synchro-

This work was done during Yucheng Lu's internship at Microsoft. [1]Department of Computer Science, Cornell University, Ithaca, NY, USA. [2]Microsoft, Redmond, WA, USA. Correspondence to: Yucheng Lu <yl2967@cornell.edu>.

Preprint. Copyright 2022 by the author(s).

[1]In the original 1-bit Adam paper, this stage is referred to as warmup stage. We use a slightly different term to avoid confusion with learning rate warmup.

nization would somehow compromise the benefits from compression or skipped rounds.

In this paper, we address these challenges by proposing **0/1 Adam**. On one hand, **0/1 Adam** leverages the insight that the variance states in adjacent Adam steps are close, and thus it can be sparsely updated and reused for several steps without having a per-step-update full-precision stage. As will be shown in Section 3 and 6, a lazily updated variance suffices to transfer the information of layer-wise adaptivity as in the original Adam. **0/1 Adam** incorporates this intuition into a design named *adaptive variance state freezing*, which effectively eliminates the need for full-precision communication and further reduces the data volume overhead in 1-bit Adam (For example, it reduces per-parameter bits from 3.27 to 1.03 on BERT-Large pretraining as shown in Section 6). To mitigate the synchronization overhead when skipping communication rounds, we make another observation that with frozen variance, the change to model parameters will be linearly dependent to the momentum state in Adam, so that if model is synchronized using 1 bit, the momentum can be approximated locally without additional communication. Given this insight, **0/1 Adam** includes another novel design, namely *1-bit sync*, that requires zero optimizer states synchronization when skipping communication rounds.

To summarize, our contributions are as follows:

- We perform a motivation study that analyzes the limitation of the state-of-the-art 1-bit Adam. (Section 3)
- Using insights from our study, we propose **0/1 Adam** that adopts two novel designs: *adaptive variance state freezing* and *1-bit sync*. (Section 4)
- We provide non-trivial convergence proofs for **0/1 Adam** on smooth and non-convex objectives. **0/1 Adam** is able to improve the convergence bound of original Adam when the variance state is sparsely updated. (Section 5)
- We conduct experiments on industrial-level model training tasks, including BERT-Base/Large pretraining and ImageNet. We demonstrate on up to 128 GPUs that **0/1 Adam** is able to reduce up to 87% of data volume, 54% of communication rounds, and achieve up to 2× higher throughput compared to the state-of-the-art 1-bit Adam without compromising end-to-end model accuracy. (Section 6)
- The 0/1 Adam optimizer and corresponding experimental scripts (e.g. BERT pre-training and GLUE finetuning) have been open sourced in a deep learning optimization library called DeepSpeed[2].

[2]https://github.com/microsoft/DeepSpeed

2. Related Work

Communication-efficient training and 1-bit compression. There has been various lines of research focusing on improving communication efficiency in large-scale training, such as using asynchrony (Niu et al., 2011; Lian et al., 2015; Xie et al., 2020), decentralization (Lian et al., 2017; Lu & De Sa, 2021), gradient quantization (Alistarh et al., 2017; Wen et al., 2017), gradient sparsification (Wangni et al., 2017; Wang et al., 2018b), local steps (Stich, 2018; Lin et al., 2018), etc. Among the most popular ones is 1-bit communication, which was first introduced in (Seide et al., 2014) to speed up speech model training, where an algorithm called 1-bit SGD is proposed. After that, Wen et al. (2017) proposes adding 0 as an additional numerical level and Liu et al. (2018) discusses the use of zero-th order oracle in 1-bit SGD. Chen et al. (2019a); Balles & Hennig (2018); Xu & Kamilov (2019) study the correlation and combination between 1-bit SGD and other techniques. Convergence analysis on 1-bit SGD is given in (Bernstein et al., 2018a; Karimireddy et al., 2019; Safaryan & Richtárik, 2021). Bernstein et al. (2018b); Sohn et al. (2019); Le Phong & Phuong (2020); Lyu (2021) investigate the robustness of 1-bit SGD. Perhaps the closest works to this paper are (Tang et al., 2021; Li et al., 2021a), which propose using two-stage training to enable 1-bit Adam and 1-bit Lamb, respectively. Among all the variants of 1-bit communication, the design with error feedback mechanism has shown to work best both empirically (Seide et al., 2014) and theoretically (Karimireddy et al., 2019). Other lines of research applies 1-bit communication to various scenarios such as federated learning (Jin et al., 2020; Yue et al., 2021), decentralized learning (Lu & De Sa, 2020; Koloskova et al., 2019), meta learning (Fan et al., 2021), etc.

Adam. Adam is an optimizer first introduced in (Kingma & Ba, 2014). It uses both first and second moment information of stochastic gradient to perform optimizer steps and has shown significant benefits on training deep learning models. Reddi et al. (2019) spots the issue of Adam convergence and provides a variant called AMSGrad while Zaheer et al. (2018) argues the Adam only converges with large batch sizes. Subsequently, other variants of Adam are proposed in (Luo et al., 2019; Chen et al., 2019b; Huang et al., 2018; Wang et al., 2019b). Multiple lines of theoretical study on Adam are given in (Fang & Klabjan, 2019; Alacaoglu et al., 2020; Défossez et al., 2020). Additionally, Chen et al. (2018); Zhou et al. (2018); Lu et al. (2020); Danilova et al. (2020); Zou et al. (2019) provide more general analysis on Adam-type optimizers.

3. 1-bit Adam and its Limitations

In this section, we introduce the background on the problem setting and illustrate the limitations and challenges from the

state-of-the-art 1-bit Adam (Tang et al., 2021).

Problem Formulation. In this paper, we consider the following optimization problem:

$$\min_{\boldsymbol{x}\in\mathbb{R}^d} f(\boldsymbol{x}) = \mathbb{E}_{\zeta\sim\mathcal{D}} f(\boldsymbol{x};\zeta). \tag{1}$$

where $\boldsymbol{x}$ denotes the d-dimensional model. $\mathcal{D}$ denotes the training set and $f(\boldsymbol{x};\zeta)$ is the loss incurred over sample ζ given model parameters $\boldsymbol{x}$. The structure of the problem naturally captures many of the model training problems.

Distributed Adam. The mathematical update rule of original distributed Adam (Kingma & Ba, 2014) can be summarized as: at step $t \geq 0$,

$$\begin{aligned}
\boldsymbol{m}_{t+1} &\leftarrow \beta_1 \boldsymbol{m}_t + (1-\beta_1)\left(1/n\sum\nolimits_{i=1}^n \boldsymbol{g}_t^{(i)}\right)\\
\boldsymbol{v}_{t+1} &\leftarrow \beta_2 \boldsymbol{v}_t + (1-\beta_2)\left(1/n\sum\nolimits_{i=1}^n \boldsymbol{g}_t^{(i)}\right)^2\\
\boldsymbol{x}_{t+1} &\leftarrow \boldsymbol{x}_t - \gamma \boldsymbol{m}_t/\sqrt{\boldsymbol{v}_t+\epsilon},
\end{aligned}$$

where n is the total number of workers and $\boldsymbol{g}_t^{(i)} = \nabla f(\boldsymbol{x}_t;\zeta_t^{(i)})$ denotes gradient estimation on worker i. $\boldsymbol{m}$ and $\boldsymbol{v}$ are two auxiliary optimizer states, which we usually refer to as momentum and variance, that captures the dynamics of first and second moment gradient estimates. γ is the learning rate, ϵ is a small constant to prevent zero division, β_1 and β_2 are decaying factors for the two states. Note that the division and square operate element-wise.

1-bit Communication. The main bottleneck in running distributed Adam is the accumulation of $1/n\sum_{i=1}^n \boldsymbol{g}_t^{(i)}$ since the gradients are usually high-dimensional. Based on the profiling results from (Tang et al., 2021; Li et al., 2021a), the communication of gradients could take up to 94% of the total training time on modern clusters. 1-bit compression (Liu et al., 2018) mitigates this problem by sending each gradient with only signs and a shared, usually the average over all the coordinates, magnitude. More specifically, denote $\mathcal{C}[\cdot]$ as the 1-bit compression, then

$$\mathcal{C}[\boldsymbol{a}] = \frac{\|\boldsymbol{a}\|_1}{d}\cdot \text{sign}(\boldsymbol{a}), \forall \boldsymbol{a}\in\mathbb{R}^d. \tag{2}$$

It is straightforward to observe that naively applying 1 bit to compress gradients in the original Adam loses coordinate-wise adaptivity since sharing magnitude makes all the coordinates-wise learning rate $\gamma/\sqrt{\boldsymbol{v}_t+\epsilon}$ the same value.

1-bit Adam and its limitations. 1-bit Adam (Tang et al., 2021), as shown in Algorithm 1, improves the naive usage of 1-bit communication by adopting a pre-conditioned variance state from running original Adam for T_0 steps first. Note that here we defer the details of 1-bit communication to Appendix A and treat it as a black-box procedure named **1bit-AllReduce** while the original full-precision AllReduce is referred to as **AllReduce**. The intuition there is that at later stage of training, the variance state becomes stable so that $\boldsymbol{v}_{T_0}$ can be a good approximation for variance state of the remaining steps. As paritally illustrated in Section 1, the full-precision stage of 1-bit Adam still presents non-trivial overhead. For instance: as illustrated in (Tang et al., 2021), when training BERT-Large on 64 GPUs using Ethernet, while the full-precision stage contains 15% of the total steps, it can take more than 50% of the entire training in terms of the wall-clock time[3]. Additionally, we profile the per-step time for BERT-Large pretraining on a Ethernet cluster[4] and observe in a single step, the fixed cost of communication can take up to 4× of the computation time. This implies when data volume per-parameter reaches its extreme in training large models at large scales, the fixed cost of communication and compression could gradually become the bottleneck that dominates the computation time.

Algorithm 1 Generic framework of applying 1-bit communication to Adam with frozen variance state. 1-bit Adam can be viewed as a special case of setting $\mathcal{T}_{\boldsymbol{v}} = \{0,\cdots,T_0-1\}$ where T_0 denotes its total number of steps in the full-precision stage.

Require: initialized model on worker i: $\boldsymbol{x}_0^{(i)}$, learning rate $\{\gamma_t\}_{t=1}^T$, $\boldsymbol{m}_0=\boldsymbol{0}$, $\boldsymbol{v}_0=\boldsymbol{0}$, total number of iterations T, decaying factor β_1, β_2 from Adam, numerical constant ϵ, variance update step index set $\mathcal{T}_{\boldsymbol{v}}$.

for $t=0,\cdots,T-1$ **do**
  Locally compute stochastic gradient $\boldsymbol{g}_t^{(i)}$ over $\boldsymbol{x}_t^{(i)}$.
  if $t\in\mathcal{T}_{\boldsymbol{v}}$ **then**
    $\overline{\boldsymbol{g}}_t$ = **AllReduce** $\left(\boldsymbol{g}_t^{(i)}\right)$.
    Set $\boldsymbol{v}_{t+1} = \beta_2\boldsymbol{v}_t + (1-\beta_2)\overline{\boldsymbol{g}}_t$.
  else
    $\overline{\boldsymbol{g}}_t$ = **1bit-AllReduce** $\left(\boldsymbol{g}_t^{(i)}\right)$.
    Set $\boldsymbol{v}_{t+1} = \boldsymbol{v}_t$.
  end if
  Update momentum: $\boldsymbol{m}_{t+1} = \beta_1\boldsymbol{m}_t + (1-\beta_1)\overline{\boldsymbol{g}}_t$.
  Update model: $\boldsymbol{x}_{t+1}^{(i)} = \boldsymbol{x}_t^{(i)} - \gamma_t\boldsymbol{m}_t/\sqrt{\boldsymbol{v}_t+\epsilon}$.
end for
return $\boldsymbol{x}_T^{(i)}, \forall i$.

4. 0/1 Adam

In this section, we give the full description of **0/1 Adam**. To better illustrate our intuition, we profile a full run of

[3]Concretely, it shows in (Tang et al., 2021) Section 7.1 that to train BERT-Large on 64 GPUs using Ethernet, the full-precision Adam takes 174.3 hours in total while 1-bit Adam takes 51.5 hours. By a simple calculation, we know that full-precision stage of 1-bit Adam takes approximately 26.37 hours while the compression stage takes 25.13 hours.

[4]The detailed profiling numbers can be found in Appendix B.

Algorithm 2 Proposed **0/1 Adam** Algorithm

Require: local model on the i-th node $\boldsymbol{x}_0^{(i)}$, learning rate $\{\gamma_t\}_{t=1}^T$, $\boldsymbol{m}_0 = \boldsymbol{0}$, $\boldsymbol{v}_0 = \boldsymbol{0}$, auxiliary buffer $\boldsymbol{u}_0 = \boldsymbol{0}$, total number of iterations T, decaying factor β_1, β_2 from Adam, numerical constant ϵ, variance update step index set $\mathcal{T}_{\boldsymbol{v}}$, synchronization step index set $\mathcal{T}_{\boldsymbol{u}}$, the most recent step with synchronization $t' = 0$.

for $t = 0, \cdots, T-1$ **do**
  Compute local stochastic gradient $\boldsymbol{g}_t^{(i)}$.
  Update momentum: $\boldsymbol{m}_{t+\frac{1}{2}}^{(i)} = \beta_1 \boldsymbol{m}_t^{(i)} + (1-\beta_1)\boldsymbol{g}_t^{(i)}$.
  Update model: $\boldsymbol{x}_{t+\frac{1}{2}}^{(i)} = \boldsymbol{x}_t^{(i)} - \gamma_t \boldsymbol{m}_t^{(i)} / \sqrt{\boldsymbol{v}_t + \epsilon}$.
  Update buffer: $\boldsymbol{u}_{t+\frac{1}{2}}^{(i)} = \boldsymbol{u}_t^{(i)} + \gamma_t \boldsymbol{m}_t^{(i)}$.
  if $t \in \mathcal{T}_{\boldsymbol{u}}$ **then**
    $\overline{\boldsymbol{u}}_{t+\frac{1}{2}}$ = **1bit-AllReduce** $\left(\boldsymbol{u}_{t+\frac{1}{2}}^{(i)}\right)$.
    Approximate momentum with compressed buffer: $\boldsymbol{m}_{t+1}^{(i)} = \overline{\boldsymbol{u}}_{t+\frac{1}{2}} / \sum_{h=t'}^{t} \gamma_h$.
    Update model with compressed buffer: $\boldsymbol{x}_{t+1}^{(i)} = \boldsymbol{x}_{t'}^{(i)} - \overline{\boldsymbol{u}}_{t+\frac{1}{2}} / \sqrt{\boldsymbol{v}_t + \epsilon}$.
    Reset the auxiliary buffer: $\boldsymbol{u}_{t+1}^{(i)} = \boldsymbol{0}$.
    Update the synchronization step: $t' = t$.
  else
    $\boldsymbol{x}_{t+1}^{(i)} = \boldsymbol{x}_{t+\frac{1}{2}}^{(i)}$; $\boldsymbol{m}_{t+1}^{(i)} = \boldsymbol{m}_{t+\frac{1}{2}}^{(i)}$; $\boldsymbol{u}_{t+1}^{(i)} = \boldsymbol{u}_{t+\frac{1}{2}}^{(i)}$.
  end if
  if $t \in \mathcal{T}_{\boldsymbol{v}}$ **then**
    $\overline{\boldsymbol{g}}_t$ = **AllReduce** $\left(\boldsymbol{g}_t^{(i)}\right)$.
    Set $\boldsymbol{v}_{t+1} = \beta_2 \boldsymbol{v}_t + (1-\beta_2)\overline{\boldsymbol{g}}_t^2$.
  else
    Set $\boldsymbol{v}_{t+1} = \boldsymbol{v}_t$.
  end if
end for
return $\boldsymbol{x}_T$.

BERT-Large pretraining with original Adam, and summarize different metrics of momentum and variance in Figure 1.

Adaptive Variance State Freezing. It is observed from Figure 1(a) that the change of variance over steps in Adam is generally smooth. While the freezing point of 1-bit Adam does capture a step where the variance can be reused for rest of the training, it is reasonable to also presume that before the freezing point, the variance within several adjacent steps will stay close due to its smoothness. This motivates us to extend the freezing policy in 1-bit Adam into an adaptive one. Starting from the beginning, we can gradually decrease the freezing frequency and let workers agree upon the freezing points from a given step index set $\mathcal{T}_{\boldsymbol{v}}$. We provide the formal description of this idea in Algorithm 1, from which the 1-bit Adam can then be viewed as a special case of setting $\mathcal{T}_{\boldsymbol{v}} = \{0, \cdots, T_0 - 1\}$.

Skipping communication rounds requires states synchronization. As will be shown in Section 6, while a well-constructed $\mathcal{T}_{\boldsymbol{v}}$ is able to reduce the per-parameter volume towards 1 bit, its end-to-end throughput improvement is limited. This happens since, as illustrated in Section 3, the fixed cost of initiating communication rounds and compression is non-negligible. This further motivates us to let Algorithm 1 work with skipped communication rounds so as to maximize its communication efficiency. As shown in previous works, performing local steps (i.e. skipping rounds) in Adam requires synchronization on the optimizer states (Yu et al., 2019; Chen et al., 2021). Specifically, since local gradients computed on each worker are different, without periodic synchronization the optimizer states on different workers will diverge from each other. As shown in Figure 1(d) and 1(b), the difference between local and global optimizer states, momentum and variance, remain constants and do not decrease to zero. The additional synchronization on momentum and variance could potentially compromise the performance gain from applying local steps.

1-bit sync. Ideally, we want a strategy that lets all the workers reach consensus on optimizer states without incurring new communication volume. Denote $\boldsymbol{x}_t^{(i)}$, $\boldsymbol{m}_t^{(i)}$, $\boldsymbol{v}_t^{(i)}$ as the model, momentum, variance on worker i at step t, respectively. Suppose all the workers are synchronized at step t', and skip all the communication rounds to step t, we obtain for any $i \in \{1, \cdots, n\}$,

$$\boldsymbol{x}_t^{(i)} = \boldsymbol{x}_{t'}^{(i)} - \sum_{k=t'}^{t-1} \frac{\gamma_k \boldsymbol{m}_k^{(i)}}{\sqrt{\boldsymbol{v}_k^{(i)} + \epsilon}}.$$

Since directly applying 1-bit compression to model parameters can easily cause divergence (Basu et al., 2020), we instead apply compression to $\boldsymbol{x}_t^{(i)} - \boldsymbol{x}_{t'}^{(i)}$ (which we refer to as model difference) given that all the workers have agreed on $\boldsymbol{x}_{t'}^{(i)}$. Compressing the model difference, on one hand, makes the compression error bounded since when the algorithm converges, the model difference will generally approach zero; on the other hand, it provides the opportunity for us to synchronize optimizer states for free as illustrated next.

The main design of 1-bit sync is leveraged from the following observation: if all the workers use the same frozen variance during a sequence of local steps, then the model difference will be linearly dependent to the momentum. So that, the momentum can be approximated locally rather than synchronized additionally based on the communicated model difference, given the premise that the change of momentum is not abrupt within close steps. Formally, if we perform 1-bit sync at step t, the updated states will be as

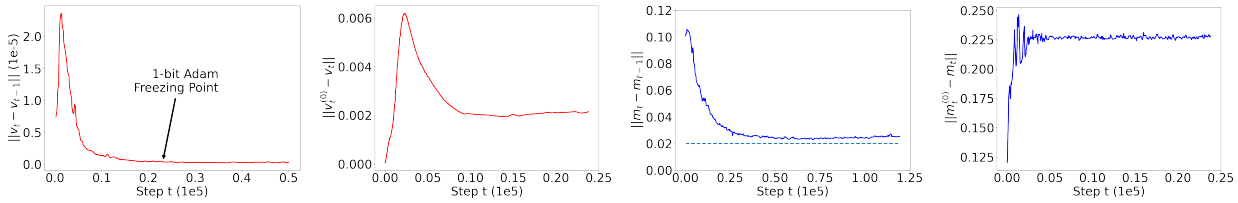

(a) $\|\boldsymbol{v}_t - \boldsymbol{v}_{t-1}\|$ over step t (b) $\|\boldsymbol{v}_t^{(0)} - \boldsymbol{v}_t\|$ over step t (c) $\|\boldsymbol{m}_t - \boldsymbol{m}_{t-1}\|$ over step t (d) $\|\boldsymbol{m}_t^{(0)} - \boldsymbol{m}_t\|$ over step t

Figure 1. Momentum and variance Profiling for BERT-Large sequence 128 pretraining with original Adam using 64 GPUs. For variance, we profile two types of metrics: the first is the difference between local and global variance: $\|\boldsymbol{v}_t^{(0)} - \boldsymbol{v}_t\|$, where $\boldsymbol{v}_t^{(0)}$ and $\boldsymbol{v}_t$ denotes the variance term computed via local gradient on worker-0 and the gradient from full-precision AllReduce, respectively. We also profile the variance difference in adjacent step $\|\boldsymbol{v}_t - \boldsymbol{v}_{t-1}\|$. Similarly, we profile the same two metrics for the momentum.

follows: with frozen variance $\boldsymbol{v}$ over all the workers,

$$\boldsymbol{u}_t^{(i)} = \sum_{k=t'}^{t} \gamma_k \boldsymbol{m}_k^{(i)} \qquad \text{(Actual sent tensor.)}$$

$$\boldsymbol{x}_{t+1}^{(i)} = \boldsymbol{x}_{t'}^{(i)} - \frac{1/n \sum_{i=1}^n \boldsymbol{u}_t^{(i)}}{\sqrt{\boldsymbol{v} + \epsilon}} \qquad \text{(Sync model params.)}$$

$$\boldsymbol{m}_{t+1}^{(i)} \approx \frac{1/n \sum_{i=1}^n \boldsymbol{u}_t^{(i)}}{\sum_{k=t'}^{t} \gamma_k} \qquad \text{(Approx. momentum.)}$$

where we omit the compression part for brevity. Combined with compression, we provide the full description of **0/1 Adam**[5] in Algorithm 2.

Techniques in 0/1 Adam are correlated. Giving a closer look at Algorithm 2, all the techniques are not orthogonally combined but are highly correlated. In fact, the approximation in 1-bit sync cannot be performed accurately if the variance during the local steps are different. On the other hand, compressing model difference rather than model itself also makes the momentum approximation possible due to their linear dependency.

5. Convergence Analysis

In this section, we provide the convergence guarantee for Algorithm 1 under arbitrary freezing policy and **0/1 Adam** (Algorithm 2) under arbitrary local steps policy. We start by making the following assumptions.

Assumption 1. Lipschitzian gradient: $f(\cdot)$ is assumed to be with L-Lipschitzian gradients, which means

$$\|\nabla f(\boldsymbol{x}) - \nabla f(\boldsymbol{y})\| \leq L\|\boldsymbol{x} - \boldsymbol{y}\|, \quad \forall \boldsymbol{x}, \forall \boldsymbol{y},$$

Assumption 2. Bounded variance: The stochastic gradient computed on each worker is unbiased and has bounded variance:

$$\mathbb{E}_{\zeta \sim \mathcal{D}} \|\nabla f(\boldsymbol{x}; \zeta) - \nabla f(\boldsymbol{x})\|^2 \leq \sigma^2, \quad \forall \boldsymbol{x}.$$

[5]The name comes from the fact that the algorithm can potentially reduce the per-parameter volume to some number between 0 and 1 bit on average.

Assumption 3. Compression error in Algorithm 1: For arbitrary $\boldsymbol{x} \in \mathbb{R}^d$, there exists a constant $0 \leq \omega < 1$, such that the output of compressor $\mathcal{C}[\cdot]$ has the following error bound:

$$\mathbb{E} \left\|\mathcal{C}[\boldsymbol{x}] - \boldsymbol{x}\right\|^2 \leq \omega \left\|\boldsymbol{x}\right\|^2.$$

Assumption 4. Bounded gradient: The infinity norm of stochastic gradient is bounded by a constant $G_\infty > 0$:

$$\|\boldsymbol{g}_t\|_\infty \leq G_\infty, \forall t.$$

Assumption 1, 2 and 4 are standard in the domain of non-convex optimization and Assumption 3 is also commonly used in compression-based optimization (Alistarh et al., 2017). Comparing with the 1-bit Adam paper (Tang et al., 2021), we do not explicitly assume the uniform lower bound on the variance coordinate, i.e., $\boldsymbol{e}_j^\top \boldsymbol{v} > v_{\min} > 0, \forall j$ for some constant $v_{\min}$. We first give the convergence theorem for Algorithm 1 as follows:

Theorem 1. *Under Assumption 1 to 4, let $m = |\mathcal{T}_{\boldsymbol{v}}|$, if we run Algorithm 1 with a constant learning rate: for all $t \geq 0$*

$$\gamma_t = \left(\sigma\sqrt{\frac{T}{n}} + \frac{\beta_2^m}{2V_1 L\sqrt{G_\infty^2 + \epsilon}} + \frac{1}{125}\right)^{-1},$$

then it holds that

$$\frac{1}{T}\sum_{t=0}^{T-1} \mathbb{E}\|\nabla f(\boldsymbol{x}_t)\|^2 \leq O\left(\frac{\beta_2^{-\frac{m}{2}}}{\sqrt{nT}} + \frac{(m+n)\beta_2^{-m}}{(1-\omega)^4 T} + \frac{1}{T}\right),$$

where we omit $f(\boldsymbol{0}) - \inf_{\boldsymbol{x}\in\mathbb{R}^d} f(\boldsymbol{x})$, G_∞, d, ϵ, σ, β_1 and L as constants.

As will be showing in Section 6, in practice we usually set $m \ll T$, and considering that β_2 is close to 1 (e.g. its default value is 0.999), m and β_2^{-m} scales as constants compared to T. Therefore, the complexity bound suggests that Algorithm 1 achieves the linear speed up, at rate $O\left(1/\sqrt{nT}\right)$, with respect to n and T. In the literature, previous works

like Zaheer et al. (2018); Défossez et al. (2020) indicate the original Adam would converge to a noise ball under constant learning rate. By comparison, Theorem 1 guarantees Algorithm 1 converges to a stationary point with arbitrary precision.

To prove the convergence for Algorithm 2, we drop Assumption 3 and instead adopt the following slightly stronger assumption.

Assumption 5. Compression error in Algorithm 2: For arbitrary $\boldsymbol{x} \in \mathbb{R}^d$, there exists a constant Δ, such that the output of compressor $\mathcal{C}[\cdot]$ has the following error bound:

$$\mathbb{E}\left\|\mathcal{C}[\boldsymbol{x}] - \boldsymbol{x}\right\|^2 \leq \Delta^2.$$

While this assumption may be strong for all step t, in practice (as will be shown in Section 6) we generally apply and increase the local steps in later part of the training, where the magnitude of momentum or model difference becomes stable. Note that this is also the assumption adopted by (Tang et al., 2021; 2019). Finally, we make a standard assumption on the upper bound of local steps:

Assumption 6. Given ordered set $\mathcal{T}_{\boldsymbol{u}}$, denote t_j as the j-th element in $\mathcal{T}_{\boldsymbol{u}}$, we assume there exists a constant $H \geq 0$, it holds that

$$\max_{1 \leq j < |\mathcal{T}_{\boldsymbol{u}}|} (t_{j+1} - t_j) \leq H.$$

The convergence for Algorithm 2 is then given in the follow theorem.

Theorem 2. *Under Assumption 1, 3, 4, 5 and 6, let $m = |\mathcal{T}_{\boldsymbol{v}}|$, if we run Algorithm 2 with a constant learning rate: for all $t \geq 0$*

$$\gamma_t = \left(\sigma\sqrt{\frac{T}{n}} + \frac{\beta_2^m}{4V_1 L\sqrt{G_\infty^2 + \epsilon}} + \frac{2\sqrt{G_\infty^2 + \epsilon}}{L} + \frac{1}{6}\right)^{-1},$$

then it holds that

$$\frac{1}{T}\sum_{t=0}^{T-1}\mathbb{E}\|\nabla f(\tilde{\boldsymbol{x}}_t)\|^2 \leq O\left(\frac{\beta_2^{-\frac{m}{2}}}{\sqrt{nT}} + \frac{H^2\Delta^2(m+n)}{\beta_2^m T} + \frac{1}{T}\right),$$

where $\tilde{\boldsymbol{x}}_t = 1/n\sum_{i=1}^n \boldsymbol{x}_t$ and we omit $f(\mathbf{0}) - \inf_{\boldsymbol{x}\in\mathbb{R}^d} f(\boldsymbol{x})$, G_∞, d, ϵ, σ, β_1 and L as constants.

Similar to Theorem 1, Algorithm 2 still achieves linear speed up, at rate $1/O(\sqrt{nT})$, given $m \ll T$ and $\beta_2 \to 1$ in practice. The effect of compression (Δ) and local steps (H) only appears on a non-dominating term.

6. Experiments

In this section we evaluate the performance of **0/1 Adam** over several industrial-level model training tasks comparing with baselines (1-bit Adam (Tang et al., 2021) and original Adam (Kingma & Ba, 2014)). Since Tang et al. (2021) already demonstrated that 1-bit Adam has similar statistical results to Adam, we omit the comparison of end-to-end model accuracy to Adam for brevity. Throughout the experiments, we enable FP16 training for all the tasks following (Tang et al., 2021). That makes the full-precision communication (including Adam, full-precision stage in 1-bit Adam and full-precision AllReduce in **0/1 Adam**) use 16-bit per number.

Dataset and models. We adopt the following tasks for the evaluation: BERT-Base ($L = 12$, $H = 768$, $A = 12$, $110M$ params) and BERT-Large ($L = 24$, $H = 1024$, $A = 16$, $340M$ params) pretraining, and training Resnet18 ($12M$ params) on ImageNet (He et al., 2016). For BERT model, we use the same dataset as (Devlin et al., 2018), which is a concatenation of Wikipedia and BooksCorpus with 2.5B and 800M words respectively. We use the GLUE fine-tuning benchmark (Wang et al., 2018a) to evaluate the convergence of the BERT models trained by different algorithms. For ImageNet, we adopt ImageNet-1k dataset, which contains 1.28M images for training and 50K images for validation (Deng et al., 2009).

Hardware. We evaluate two clusters: one with 4 NVIDIA V100 GPUs per node and 40 Gigabit Ethernet inter-node network (2.7 Gbps effective bandwidth); the other one with 8 V100 GPUs per node and 100 Gigabit InfiniBand EDR inter-node network (close to theoretical peak effective bandwidth). We use 4 to 128 GPUs for BERT and ImageNet pretraining tasks to measure **0/1 Adam**'s performance gain. Additionally, for ImageNet training we apply the accelerated data loading technique from lmdb[6].

Training Parameters. For BERT pretraining, we follow the settings from (Devlin et al., 2018) and let the learning rate linearly increases to 4×10^{-4} as a warmup in the first 12.5K steps, then decays into 0.99 of the original after every 520 steps. We set $\beta_1 = 0.9$ and $\beta_2 = 0.999$ for all the algorithms. We adopt the batch size of 4096. For 1-bit Adam, we follow the hyperparameters given in (Tang et al., 2021) and set the full-precision stage for 1-bit Adam as 16K and 23K on BERT-Base and BERT-Large, respectively. All the hyperparameters used here (e.g. learning rate) strictly follow (Tang et al., 2021) for fair comparison. For ImageNet, we follow the example script from Pytorch[7] and use batch size of 256 and a milestone decay learning rate schedule: starting at 1e-4 and decay by a factor of 10 at epoch 30 and 60, with 90 epochs in total. We set 10 epochs (50050 steps) as the full-precision stage for 1-bit Adam.

[6] https://github.com/xunge/pytorch_lmdb_imagenet

[7] https://github.com/pytorch/examples/blob/master/imagenet/main.py

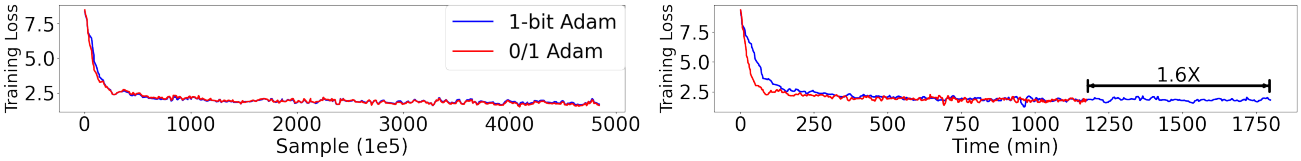

(a) BERT-Base pretraining seq128

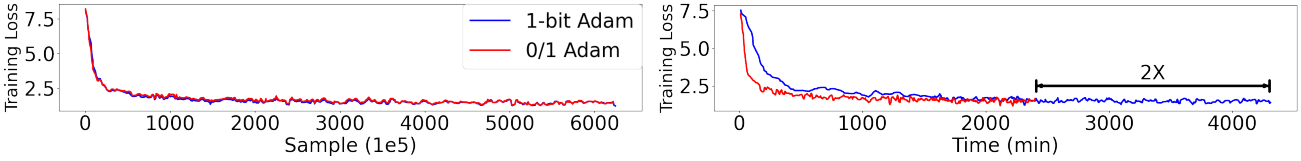

(b) BERT-Large pretraining seq128

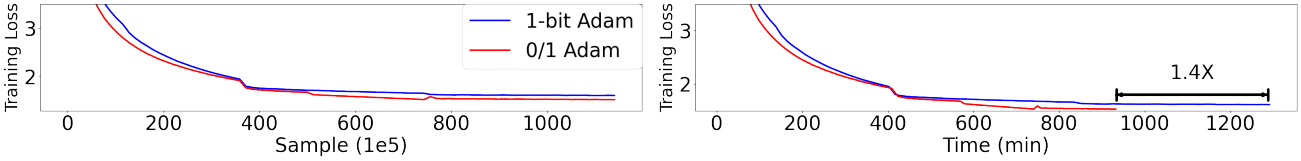

(c) Resnet18 on ImageNet

Figure 2. Sample-wise and time-wise convergence for BERT-Base/Large pre-training sequence length 128 and Resnet18 pretraining on ImageNet using 128 GPUs on the Ethernet cluster.

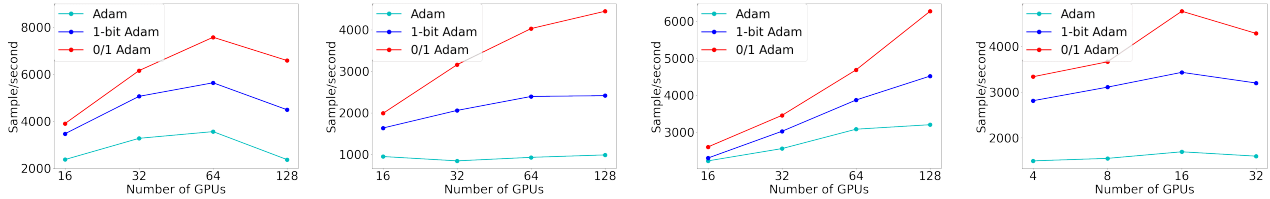

(a) BERT-Base (Ethernet) batch size=4096

(b) BERT-Large (Ethernet) batch size=4096

(c) BERT-Large (InfiniBand) batch size=4096

(d) ImageNet (Ethernet) batch size=256

Figure 3. End-to-end average throughput for BERT-Base/Large pre-training sequence length 128 and Resnet18 pretraining on ImageNet using 128 V100 GPUs on the Ethernet/InfiniBand cluster. Note that since for ImageNet, both batch size (256) and model (Resnet18) are small compared to BERT, and its parallelism speed up will be limited if applied to the same large system on BERT (128 GPUs). And so we test it for 4 to 32 GPUs in Figure (d).

For GLUE benchmarks we use Adam optimizer and perform single-task training on the dev set. Following the setup in the BERT paper (Devlin et al., 2018) and 1-bit Adam paper (Tang et al., 2021), we search over the hyperparameter space with batch sizes $\in \{8, 16, 32\}$ and learning rates $\{1 \times 10^{-5}, 3 \times 10^{-5}, 5 \times 10^{-5}, 8 \times 10^{-5}\}$.

Policy for $\mathcal{T}_v$ and $\mathcal{T}_u$ in 0/1 Adam. We first illustrate our policy on $\mathcal{T}_v$. Observing from our motivation study (Figure 1) that the variance difference in adjacent steps decreases roughly exponentially. Denote k_j as the step where j-th variance update takes place, we select $\mathcal{T}_v$ such that,

$$k_{j+1} - k_j = 2^{\lfloor j/\kappa \rfloor}, \forall \kappa > 0.$$

We adopt $\kappa = 16$ for all the three tasks.

Then we move on to discuss the policy for $\mathcal{T}_u$. Based on the derivation in Section 4, the approximation noise from local step is proportional to the learning rate. And so if we denote t_j as the step where j-th synchronization takes place, then our intuition is to increase $t_{j+1} - t_j$ roughly inversely proportional to the learning rate at t_j so as to make the approximation noise bounded. For BERT-Base/Large pretraining, as illustrated before, the learning rate exponentially decreases by 0.99 every 520 steps after 12.5K linear increase warmup steps. So that we set $t_{j+1} - t_j = 1$ for the first 12.5K steps and after that let it multiply by 2 every 32678 steps based on the calculation that the learning rate will decrease by half. Similarly, for ImageNet we set $t_{j+1} - t_j = 1$ for the first 50050 steps (10 epochs) and after that let it multiply by 2 every 50050 steps (10 epochs). We clip the interval at 16 in all the tasks. This corresponds to $H = 16$ in Assumption 6.Finally, since our theory in Section 5 indicates that approximation will be more accurate when the variance is frozen. So that we additionally stop

Table 1. GLUE development set results. BERT-Base/Large(original) results are from (Devlin et al., 2018). BERT-Base/Large(1-bit Adam) results are from (Tang et al., 2021). The scores are the median scores over 10 runs with different seeds. The scores are obtained on the checkpoints trained by both sequence 128 and sequence 512 datasets.

	RTE	MRPC	STS-B	CoLA	SST-2	QNLI	QQP	MNLI-(m/mm)	Avg Score
BERT-Base(Original)	66.4	84.8	85.8	52.1	93.5	90.5	89.2	84.6/83.4	81.1
BERT-Base(1-bit Adam)	69.0	84.8	83.6	55.6	91.6	90.8	90.9	83.6/83.9	81.5
BERT-Base(**0/1 Adam**)	69.7	85.1	84.9	54.4	91.9	90.3	90.7	83.7/83.7	81.6
BERT-Large(Original)	70.1	85.4	86.5	60.5	94.9	92.7	89.3	86.7/85.9	83.6
BERT-Large(1-bit Adam)	70.4	86.1	86.1	62.0	93.8	91.9	91.5	85.7/85.4	83.7
BERT-Large(**0/1 Adam**)	71.7	86.2	86.9	59.9	93.2	91.6	91.4	85.6/85.6	83.6

Table 2. Top1 accuracy of the output models at the end of epoch 90 from different algorithms. The original accuracy is provided by Pytorch pretrained model library (Pytorch, 2014). For the other two algorithms, the accuracy is the highest score over 3 runs.

	Top1 Acc.
Original	69.76
1-bit Adam	69.93
0/1 Adam	69.88

updating variance when $t_{j+1} - t_j > 1$.

6.1. Convergence Analysis

Figure 2 presents the sample-wise and time-wise convergence results for different algorithms with 128 GPUs on the Ethernet cluster. We find that **0/1 Adam** provides the same sample-wise convergence speed compared to the baseline, with up to 2× time-wise speed up. Table 1 summarizes the GLUE results using the checkpoints from our BERT pretraining experiments. **0/1 Adam** achieves similar accuracy compared to the numbers reported in previous work. Table 2 provides the ImageNet validation accuracy of trained models from different algorithms, and we find the final accuracy can achieve the reported accuracy from Pytorch library (Pytorch, 2014).

6.2. Throughput Analysis

Figure 3 summarizes the throughput results on different tasks and different clusters. We observe that **0/1 Adam** can consistently outperform baselines in all settings. It is also worth mentioning that **0/1 Adam** on Ethernet (2.7 Gbps effective bandwidth, 4 GPUs per node) is able to achieve comparable throughput as 1-bit Adam on InfiniBand (near 100 Gbps effective bandwidth, 8 GPUs per node), as shown in the red line in Figure 3(b) and the blue line in Figure 3(c), which demonstrates **0/1 Adam** further removes the redundancy in communication effectively that exceeds the hardware barrier.

Communication reduction and the role of skipping rounds. To better understand the importance and effect

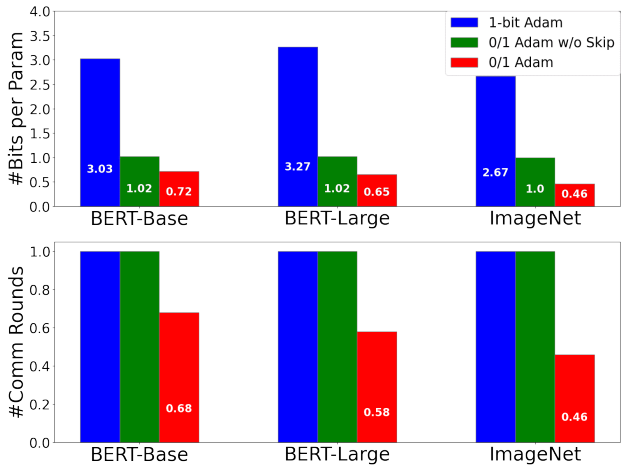

Figure 4. Reduction on number of bits per parameter used and number of communication rounds in different tasks. Note that the communication round numbers are normalized due to scale difference in different tasks.

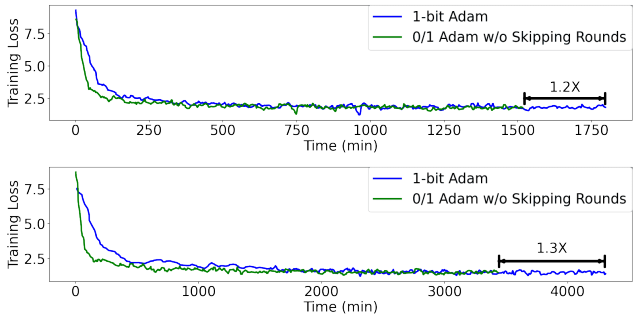

Figure 5. Evaluation BERT-Base/Large pretraining throughput using **0/1 Adam** without communication rounds skipping. Comparing with Figure 4 and 2, skipping rounds breaks the barrier on the performance gain.

of skipping communication rounds, we additionally run a special case of **0/1 Adam** where we keep the same policy of $\mathcal{T}_v$ but use $\mathcal{T}_u = \{0, \cdots, T-1\}$. This special version of **0/1 Adam** does not skip rounds but use the same variance freezing policy. We plot the data volume usage and throughput results in Figure 4 and 5, respectively. We see that although no skipping rounds suffice to reduce the data volume overhead from 1-bit Adam towards 1-bit-per-parameter

in general, the throughput improvement is limited compared to Figure 2. This again suggests that skipping rounds and the design of 1-bit sync is crucial to performance gain.

7. Conclusion

In this paper, we study the challenges of using 1-bit communication on Adam, and limitations of the state-of-the-art 1-bit Adam algorithm. We propose an algorithm named **0/1 Adam** that adopts two novel design: adaptive variance state freezing and 1-bit sync. We provide convergence proof for **0/1 Adam** and measure its effectiveness over baseline Adam and 1-bit Adam on various benchmarks, including BERT-Base/Large pretraining and ImageNet.

References

Alacaoglu, A., Malitsky, Y., Mertikopoulos, P., and Cevher, V. A new regret analysis for adam-type algorithms. In *International Conference on Machine Learning*, pp. 202–210. PMLR, 2020.

Alistarh, D., Grubic, D., Li, J., Tomioka, R., and Vojnovic, M. Qsgd: Communication-efficient sgd via gradient quantization and encoding. *Advances in Neural Information Processing Systems*, 30:1709–1720, 2017.

Balles, L. and Hennig, P. Dissecting adam: The sign, magnitude and variance of stochastic gradients. In *International Conference on Machine Learning*, pp. 404–413. PMLR, 2018.

Basu, D., Data, D., Karakus, C., and Diggavi, S. N. Qsparse-local-sgd: Distributed sgd with quantization, sparsification, and local computations. *IEEE Journal on Selected Areas in Information Theory*, 1(1):217–226, 2020.

Bernstein, J., Wang, Y.-X., Azizzadenesheli, K., and Anandkumar, A. signsgd: Compressed optimisation for non-convex problems. In *International Conference on Machine Learning*, pp. 560–569. PMLR, 2018a.

Bernstein, J., Zhao, J., Azizzadenesheli, K., and Anandkumar, A. signsgd with majority vote is communication efficient and fault tolerant. *arXiv preprint arXiv:1810.05291*, 2018b.

Chen, X., Liu, S., Sun, R., and Hong, M. On the convergence of a class of adam-type algorithms for non-convex optimization. *arXiv preprint arXiv:1808.02941*, 2018.

Chen, X., Chen, T., Sun, H., Wu, Z. S., and Hong, M. Distributed training with heterogeneous data: Bridging median-and mean-based algorithms. *arXiv preprint arXiv:1906.01736*, 2019a.

Chen, X., Liu, S., Xu, K., Li, X., Lin, X., Hong, M., and Cox, D. Zo-adamm: Zeroth-order adaptive momentum method for black-box optimization. *arXiv preprint arXiv:1910.06513*, 2019b.

Chen, X., Karimi, B., Zhao, W., and Li, P. On the convergence of decentralized adaptive gradient methods. *arXiv preprint arXiv:2109.03194*, 2021.

Danilova, M., Dvurechensky, P., Gasnikov, A., Gorbunov, E., Guminov, S., Kamzolov, D., and Shibaev, I. Recent theoretical advances in non-convex optimization. *arXiv preprint arXiv:2012.06188*, 2020.

Défossez, A., Bottou, L., Bach, F., and Usunier, N. A simple convergence proof of adam and adagrad. *arXiv preprint arXiv:2003.02395*, 2020.

Deng, J., Dong, W., Socher, R., Li, L.-J., Li, K., and Fei-Fei, L. Imagenet: A large-scale hierarchical image database. In *2009 IEEE conference on computer vision and pattern recognition*, pp. 248–255. Ieee, 2009.

Devlin, J., Chang, M.-W., Lee, K., and Toutanova, K. Bert: Pre-training of deep bidirectional transformers for language understanding. *arXiv preprint arXiv:1810.04805*, 2018.

Fan, C., Ram, P., and Liu, S. Sign-maml: Efficient model-agnostic meta-learning by signsgd. *arXiv preprint arXiv:2109.07497*, 2021.

Fang, B. and Klabjan, D. Convergence analyses of online adam algorithm in convex setting and two-layer relu neural network. *arXiv preprint arXiv:1905.09356*, 2019.

He, K., Zhang, X., Ren, S., and Sun, J. Deep residual learning for image recognition. In *Proceedings of the IEEE conference on computer vision and pattern recognition*, pp. 770–778, 2016.

Huang, H., Wang, C., and Dong, B. Nostalgic adam: Weighting more of the past gradients when designing the adaptive learning rate. *arXiv preprint arXiv:1805.07557*, 2018.

Jin, R., Huang, Y., He, X., Dai, H., and Wu, T. Stochastic-sign sgd for federated learning with theoretical guarantees. *arXiv preprint arXiv:2002.10940*, 2020.

Karimireddy, S. P., Rebjock, Q., Stich, S., and Jaggi, M. Error feedback fixes signsgd and other gradient compression schemes. In *International Conference on Machine Learning*, pp. 3252–3261. PMLR, 2019.

Kingma, D. P. and Ba, J. Adam: A method for stochastic optimization. *arXiv preprint arXiv:1412.6980*, 2014.

Koloskova, A., Lin, T., Stich, S. U., and Jaggi, M. Decentralized deep learning with arbitrary communication compression. *arXiv preprint arXiv:1907.09356*, 2019.

Le Phong, T. and Phuong, T. T. Distributed signsgd with improved accuracy and network-fault tolerance. *IEEE Access*, 8:191839–191849, 2020.

Li, C., Awan, A. A., Tang, H., Rajbhandari, S., and He, Y. 1-bit lamb: Communication efficient large-scale large-batch training with lamb's convergence speed. *arXiv preprint arXiv:2104.06069*, 2021a.

Li, C., Zhang, M., and He, Y. Curriculum learning: A regularization method for efficient and stable billion-scale gpt model pre-training. *arXiv preprint arXiv:2108.06084*, 2021b.

Lian, X., Huang, Y., Li, Y., and Liu, J. Asynchronous parallel stochastic gradient for nonconvex optimization. *Advances in Neural Information Processing Systems*, 28: 2737–2745, 2015.

Lian, X., Zhang, C., Zhang, H., Hsieh, C.-J., Zhang, W., and Liu, J. Can decentralized algorithms outperform centralized algorithms? a case study for decentralized parallel stochastic gradient descent. *arXiv preprint arXiv:1705.09056*, 2017.

Lin, T., Stich, S. U., Patel, K. K., and Jaggi, M. Don't use large mini-batches, use local sgd. *arXiv preprint arXiv:1808.07217*, 2018.

Liu, S., Chen, P.-Y., Chen, X., and Hong, M. signsgd via zeroth-order oracle. In *International Conference on Learning Representations*, 2018.

Lu, Y. and De Sa, C. Moniqua: Modulo quantized communication in decentralized sgd. In *International Conference on Machine Learning*, pp. 6415–6425. PMLR, 2020.

Lu, Y. and De Sa, C. Optimal complexity in decentralized training. In *International Conference on Machine Learning*, pp. 7111–7123. PMLR, 2021.

Lu, Y., Nash, J., and De Sa, C. Mixml: A unified analysis of weakly consistent parallel learning. *arXiv preprint arXiv:2005.06706*, 2020.

Luo, L., Xiong, Y., Liu, Y., and Sun, X. Adaptive gradient methods with dynamic bound of learning rate. *arXiv preprint arXiv:1902.09843*, 2019.

Lyu, L. Dp-signsgd: When efficiency meets privacy and robustness. In *ICASSP 2021-2021 IEEE International Conference on Acoustics, Speech and Signal Processing (ICASSP)*, pp. 3070–3074. IEEE, 2021.

Niu, F., Recht, B., Ré, C., and Wright, S. J. Hogwild!: A lock-free approach to parallelizing stochastic gradient descent. *arXiv preprint arXiv:1106.5730*, 2011.

Pytorch. Torchvision 0.11.0 documentation — pytorch.org. https://pytorch.org/vision/stable/models.html, 2014.

Radford, A., Wu, J., Amodei, D., Amodei, D., Clark, J., Brundage, M., and Sutskever, I. Better language models and their implications. *OpenAI blog*, 1:2, 2019.

Reddi, S. J., Kale, S., and Kumar, S. On the convergence of adam and beyond. *arXiv preprint arXiv:1904.09237*, 2019.

Safaryan, M. and Richtárik, P. Stochastic sign descent methods: New algorithms and better theory. In *International Conference on Machine Learning*, pp. 9224–9234. PMLR, 2021.

Seide, F., Fu, H., Droppo, J., Li, G., and Yu, D. 1-bit stochastic gradient descent and its application to data-parallel distributed training of speech dnns. In *Fifteenth Annual Conference of the International Speech Communication Association*. Citeseer, 2014.

Shoeybi, M., Patwary, M., Puri, R., LeGresley, P., Casper, J., and Catanzaro, B. Megatron-lm: Training multi-billion parameter language models using model parallelism. *arXiv preprint arXiv:1909.08053*, 2019.

Sohn, J.-y., Han, D.-J., Choi, B., and Moon, J. Election coding for distributed learning: Protecting signsgd against byzantine attacks. *arXiv preprint arXiv:1910.06093*, 2019.

Stich, S. U. Local sgd converges fast and communicates little. *arXiv preprint arXiv:1805.09767*, 2018.

Tang, H., Yu, C., Lian, X., Zhang, T., and Liu, J. Doublesqueeze: Parallel stochastic gradient descent with double-pass error-compensated compression. In *International Conference on Machine Learning*, pp. 6155–6165. PMLR, 2019.

Tang, H., Gan, S., Awan, A. A., Rajbhandari, S., Li, C., Lian, X., Liu, J., Zhang, C., and He, Y. 1-bit adam: Communication efficient large-scale training with adam's convergence speed. *arXiv preprint arXiv:2102.02888*, 2021.

Trinh, T. H. and Le, Q. V. A simple method for commonsense reasoning. *arXiv preprint arXiv:1806.02847*, 2018.

Wang, A., Singh, A., Michael, J., Hill, F., Levy, O., and Bowman, S. R. Glue: A multi-task benchmark and analysis platform for natural language understanding. *arXiv preprint arXiv:1804.07461*, 2018a.

Wang, D., Liu, Y., Tang, W., Shang, F., Liu, H., Sun, Q., and Jiao, L. signadam++: Learning confidences for deep neural networks. In *2019 International Conference on Data Mining Workshops (ICDMW)*, pp. 186–195. IEEE, 2019a.

Wang, G., Lu, S., Tu, W., and Zhang, L. Sadam: A variant of adam for strongly convex functions. *arXiv preprint arXiv:1905.02957*, 2019b.

Wang, H., Sievert, S., Charles, Z., Liu, S., Wright, S., and Papailiopoulos, D. Atomo: Communication-efficient learning via atomic sparsification. *arXiv preprint arXiv:1806.04090*, 2018b.

Wangni, J., Wang, J., Liu, J., and Zhang, T. Gradient sparsification for communication-efficient distributed optimization. *arXiv preprint arXiv:1710.09854*, 2017.

Wen, W., Xu, C., Yan, F., Wu, C., Wang, Y., Chen, Y., and Li, H. Terngrad: Ternary gradients to reduce communication in distributed deep learning. *arXiv preprint arXiv:1705.07878*, 2017.

Xie, C., Koyejo, S., and Gupta, I. Zeno++: Robust fully asynchronous sgd. In *International Conference on Machine Learning*, pp. 10495–10503. PMLR, 2020.

Xu, X. and Kamilov, U. S. Signprox: One-bit proximal algorithm for nonconvex stochastic optimization. In *ICASSP 2019-2019 IEEE International Conference on Acoustics, Speech and Signal Processing (ICASSP)*, pp. 7800–7804. IEEE, 2019.

Yu, H., Jin, R., and Yang, S. On the linear speedup analysis of communication efficient momentum sgd for distributed non-convex optimization. In *International Conference on Machine Learning*, pp. 7184–7193. PMLR, 2019.

Yue, K., Jin, R., Wong, C.-W., and Dai, H. Federated learning via plurality vote. *arXiv preprint arXiv:2110.02998*, 2021.

Zaheer, M., Reddi, S., Sachan, D., Kale, S., and Kumar, S. Adaptive methods for nonconvex optimization. *Advances in neural information processing systems*, 31, 2018.

Zellers, R., Holtzman, A., Rashkin, H., Bisk, Y., Farhadi, A., Roesner, F., and Choi, Y. Defending against neural fake news. *Advances in neural information processing systems*, 32, 2019.

Zhou, D., Chen, J., Cao, Y., Tang, Y., Yang, Z., and Gu, Q. On the convergence of adaptive gradient methods for nonconvex optimization. *arXiv preprint arXiv:1808.05671*, 2018.

Zou, F., Shen, L., Jie, Z., Zhang, W., and Liu, W. A sufficient condition for convergences of adam and rmsprop. In *Proceedings of the IEEE/CVF Conference on Computer Vision and Pattern Recognition*, pp. 11127–11135, 2019.

A. Full Description to AllReduce and 1-bit AllReduce

As introduced in Section 2, the error feedback based **1bit-AllReduce** works best both in theory and in practice. In fact, the original 1-bit Adam also adopts the error-feedback design (Tang et al., 2021). We give the full description of this **1bit-AllReduce** in Algorithm 3. In the theoretical analysis, our proofs will also rely on this algorithm. Note that this algorithm does not require any additional assumptions for our theory to hold, since this fits the black-box procedure in Algorithm 1 and Algorithm 2.

Algorithm 3 The full description of Error Feedback 1 bit Communication (**1bit-AllReduce**)

Require: communication buffer $\boldsymbol{z}_t^{(i)}$, worker error $\boldsymbol{\delta}_t^{(i)}$, server error $\overline{\boldsymbol{\delta}}_t$, 1-bit compressor $\mathcal{C}[\cdot]$. Both worker and server errors will be initialized at $\mathbf{0}$ at $t = 0$.

1: **(On i-th node)**
2: Compress $\boldsymbol{z}_t^{(i)}$ into $\hat{\boldsymbol{z}}_t^{(i)} = \mathcal{C}[\boldsymbol{z}_t^{(i)} + \boldsymbol{\delta}_t^{(i)}]$, and update the compression error by $\boldsymbol{\delta}_{t+1}^{(i)} = \boldsymbol{z}_t^{(i)} + \boldsymbol{\delta}_t^{(i)} - \hat{\boldsymbol{z}}_t^{(i)}$.
3: Send $\hat{\boldsymbol{z}}_t^{(i)}$ to the server.
4: **(On server)**
5: Take the average over all the $\hat{\boldsymbol{z}}_t^{(i)}$ and compress it into $\overline{\boldsymbol{z}}_t = \mathcal{C}[\frac{1}{n}\sum_{i=1}^n \hat{\boldsymbol{z}}_{t+1}^{(i)} + \overline{\boldsymbol{\delta}}_t]$, and update the compression error by $\overline{\boldsymbol{\delta}}_{t+1} = \frac{1}{n}\sum_{i=1}^n \hat{\boldsymbol{z}}_t^{(i)} + \overline{\boldsymbol{\delta}}_t - \overline{\boldsymbol{z}}_t$.
6: Send $\overline{\boldsymbol{z}}_t$ to all the workers.
7: **(On i-th node)**
8: **return** $\overline{\boldsymbol{z}}_t$, $\boldsymbol{\delta}_{t+1}^{(i)}$, $\overline{\boldsymbol{\delta}}_{t+1}$.

Algorithm 4 The full description of **AllReduce**

Require: communication buffer $\boldsymbol{z}_t^{(i)}$.

1: **(On i-th node)**
2: Send $\boldsymbol{z}_t^{(i)}$ to the server.
3: **(On server)**
4: Take the average over all the $\boldsymbol{z}_t^{(i)}$ into $\overline{\boldsymbol{z}}_t = \frac{1}{n}\sum_{i=1}^n \boldsymbol{z}_t^{(i)}$.
5: Send $\overline{\boldsymbol{z}}_t$ to all the workers.
6: **(On i-th node)**
7: **return** $\overline{\boldsymbol{z}}_t$.

B. Profiling Results for Fixed Cost of Communication

Table 3. Profiling on Ethernet cluster the time taken in computation and others (including initialization of a communication round and compression) during one 1-bit AllReduce round at different scales.

Resnet18/ImageNet	4 node (16 GPUs)	8 node (32 GPUs)	16 node (64 GPUs)	32 node (128 GPUs)
Computation	73ms	68ms	44ms	51ms
Others	8ms	6ms	21ms	19ms
BERT-Base	4 node (16 GPUs)	8 node (32 GPUs)	16 node (64 GPUs)	32 node (128 GPUs)
Computation	941ms	490ms	263ms	162ms
Others	153ms	250ms	397ms	658ms
BERT-Large	4 node (16 GPUs)	8 node (32 GPUs)	16 node (64 GPUs)	32 node (128 GPUs)
Computation	1840ms	970ms	640ms	332ms
Others	340ms	510ms	590ms	931ms

C. Additional Results on GPT-2

In this section, we provide additional results over GPT-2 pretraining. We adopt a GPT-2 model from its original paper (Radford et al., 2019), which contains 117M parameters (48 layers, 1600 hidden size, 25 attention heads). For training data,

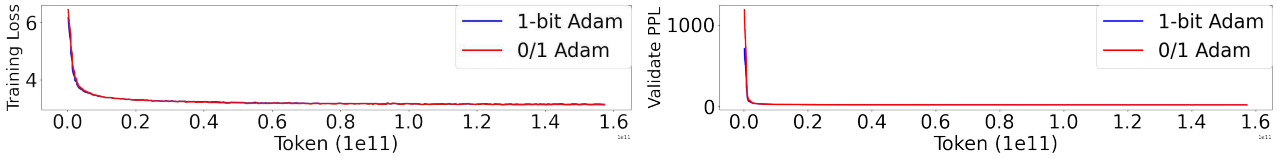

Figure 6. Training loss (left) and validation perplexity (right) with respect to Tokens for 1-bit Adam and **0/1 Adam**.

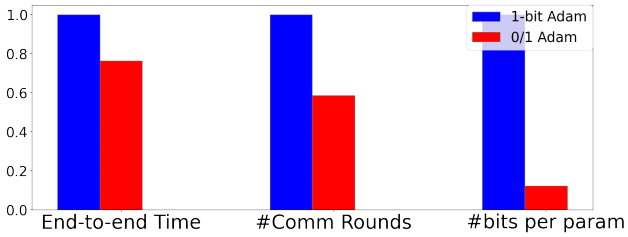

Figure 7. Reduction on different metrics for 1-bit Adam and **0/1 Adam**. Note that the figures are normalized due to the scale difference on three metrics. The specific numbers for the three metrics (from left to right, with the order of 1-bit Adam/**0/1 Adam**) are: 34.52/26.29 hours, 300K/175K rounds, 5.0/0.61 bits, respectively.

we adopt the same dataset blend as in (Shoeybi et al., 2019): Wikipedia (Devlin et al., 2018), CC-Stories (Trinh & Le, 2018), RealNews (Zellers et al., 2019), and OpenWebtext (Radford et al., 2019).

We set batch size to be 512, and use 300K training steps (158B tokens). The learning rate schedule follows a linear warmup of 3K steps and a single cycle consine decay over the remaining 297K steps (1×10^{-5} min). For 1-bit Adam, we set its full-precision stage length to be 80K steps, and for the **0/1 Adam**, we follow the same learning rate based policy from BERT on $\mathcal{T}_{\boldsymbol{v}}$ and $\mathcal{T}_{\boldsymbol{u}}$. Both algorithms run on a 64-GPU Infiniband cluster.

Table 4. Zero-shot evaluation of the trained models on WikiText-103 and LAMBADA datasets, the evaluation methodology follows (Shoeybi et al., 2019). The number for Adam is obtained from (Li et al., 2021b).

	WikiText Perplexity ↓	LAMBADA accuracy ↑
Adam	27.78	33.19
1-bit Adam	28.37	33.21
0/1 Adam	28.07	33.51

Figure 6 and Figure 7 show that **0/1 Adam** is able to achieve the same convergence speed as 1-bit Adam with less communication rounds and bits per parameters, which is aligned with our findings on BERT and ImageNet tasks. Table 4 summarizes the quality of output models via zero-shot tasks over WikiText-103 and LAMBADA datasets. We observe **0/1 Adam** is able to achieve the comparable perplexity and accuracy with Adam, while higher than 1-bit Adam.

D. Theoretical Analysis

D.1. Proof to Theorem 1

Note that the following proof will use Algorithm 3 to replace **1bit-AllReduce** in Algorithm 1, as introduced in Section A.

Proof. The main update of Algorithm 1 (with constant learning rate) can be summarized as: for every $t = 0, \cdots, T-1$,

$$\boldsymbol{m}_{t+1} = \beta_1 \boldsymbol{m}_t + (1-\beta_1)\overline{\boldsymbol{g}}_t$$

$$\boldsymbol{v}_{t+1} = \begin{cases} \beta_2 \boldsymbol{v}_t + (1-\beta_2)\left(\frac{1}{n}\sum_{i=1}^n \boldsymbol{g}_t^{(i)}\right)^2 & t \in \mathcal{T}_{\boldsymbol{v}}, \\ \boldsymbol{v}_t & t \notin \mathcal{T}_{\boldsymbol{v}}. \end{cases}$$

$$\boldsymbol{x}_{t+1} = \boldsymbol{x}_t - \gamma \frac{\boldsymbol{m}_t}{\sqrt{\boldsymbol{v}_t + \epsilon}},$$

where the $\overline{\boldsymbol{g}}_t$ is the output of the **1-bit AllReduce** algorithm[8]. Note that based on Algorithm 3, the gradient approximation term follows:

$$\begin{aligned}
\overline{\boldsymbol{g}}_t =& \frac{1}{n}\sum_{i=1}^{n} \hat{\boldsymbol{g}}_t^{(i)} + \overline{\boldsymbol{\delta}}_t - \overline{\boldsymbol{\delta}}_{t+1} \\
=& \frac{1}{n}\sum_{i=1}^{n} \left(\boldsymbol{g}_t^{(i)} + \boldsymbol{\delta}_t^{(i)} - \boldsymbol{\delta}_{t+1}^{(i)}\right) + \overline{\boldsymbol{\delta}}_t - \overline{\boldsymbol{\delta}}_{t+1} \\
=& \frac{1}{n}\sum_{i=1}^{n} \boldsymbol{g}_t^{(i)} + \left(\frac{1}{n}\sum_{i=1}^{n} \boldsymbol{\delta}_t^{(i)} - \overline{\boldsymbol{\delta}}_t\right) - \left(\frac{1}{n}\sum_{i=1}^{n} \boldsymbol{\delta}_{t+1}^{(i)} - \overline{\boldsymbol{\delta}}_{t+1}\right) \\
=& \boldsymbol{g}_t + \boldsymbol{\delta}_t - \boldsymbol{\delta}_{t+1},
\end{aligned}$$

where we denote

$$\begin{aligned}
\boldsymbol{g}_t =& \frac{1}{n}\sum_{i=1}^{n} \boldsymbol{g}_t^{(i)} \\
\boldsymbol{\delta}_t =& \frac{1}{n}\sum_{i=1}^{n} \boldsymbol{\delta}_t^{(i)} - \overline{\boldsymbol{\delta}}_t.
\end{aligned}$$

To prove the convergence, we now define the following auxiliary sequence: for any $t \geq 0$,

$$\boldsymbol{y}_t = \boldsymbol{x}_t - \frac{\gamma \boldsymbol{m}_t}{(1-\beta_1)\sqrt{\boldsymbol{v}_t + \epsilon}} - \frac{\gamma \boldsymbol{\delta}_t}{\sqrt{\boldsymbol{v}_t + \epsilon}}.$$

The rest of the proof is to use this auxiliary sequence to bound two types of steps separately. We call a step t as *reuse step* if $t \notin \mathcal{T}_{\boldsymbol{v}}$ and *update step* otherwise. We see for all the update steps, $\boldsymbol{v}_t \neq \boldsymbol{v}_{t+1}$ while for all the reuse steps $\boldsymbol{v}_t = \boldsymbol{v}_{t+1}$. The bounds on two different types of steps are provides by Lemma 5 and Lemma 6. Specifically, denoting $V_1 = \left\| \frac{1}{\sqrt{\boldsymbol{v}_1 + \epsilon}} \right\|_1$, from Lemma 5 we obtain for all the reuse steps,

$$\begin{aligned}
\sum_{t \notin \mathcal{T}_{\boldsymbol{v}}} \frac{\gamma}{4\sqrt{G_\infty^2 + \epsilon}} \mathbb{E}\|\nabla f(\boldsymbol{x}_t)\|^2 \leq& \sum_{t \notin \mathcal{T}_{\boldsymbol{v}}} \mathbb{E}[f(\boldsymbol{y}_t) - f(\boldsymbol{y}_{t+1})] + \frac{227\gamma^3 L^2 V_1^2 (1+\omega)^3 G_\infty^2 d\sqrt{G_\infty^2 + \epsilon}(T-m)}{\beta_2^{2m}(1-\beta_1)^2(1-\omega)^4} \\
&+ \frac{L\gamma^2\sigma^2 V_1 (T-m)}{2n\beta_2^m}.
\end{aligned}$$

while from Lemma 6 we obtain for all the update steps,

$$\begin{aligned}
\sum_{t \in \mathcal{T}_{\boldsymbol{v}}} \frac{\gamma}{4\sqrt{G_\infty^2 + \epsilon}} \mathbb{E}\|\nabla f(\boldsymbol{x}_t)\|^2 \leq& \sum_{t \in \mathcal{T}_{\boldsymbol{v}}} \mathbb{E}[f(\boldsymbol{y}_t) - f(\boldsymbol{y}_{t+1})] + \left(\frac{34\gamma}{L} + \frac{\gamma}{4\sqrt{G_\infty^2 + \epsilon}}\right) \cdot \left(\frac{\sigma^2}{n} + G_\infty^2 d\right) m \\
&+ \frac{32\gamma(1+\beta_1)^2(1+\omega)^3 V_1 G_\infty^2 dmL}{\beta_2^m (1-\beta_1)^2 (1-\omega)^4}.
\end{aligned}$$

Note that the two inequalities above hold when the learning rate fulfills

$$\gamma \leq \min\left\{ \frac{\beta_2^m}{2V_1 L\sqrt{G_\infty^2 + \epsilon}}, \frac{1}{125} \right\}.$$

[8] In the original Algorithm 1, the $\overline{\boldsymbol{g}}_t$ is the output of the **AllReduce** when $t \in \mathcal{T}_{\boldsymbol{v}}$. This, however, does not affect our analysis, since our proof holds for a noisier case. The original Algorithm 1 is mainly for practical concern – we avoid redundant **AllReduce** rounds when **1-bit AllReduce** is performed.

Combine them together,

$$\frac{1}{T}\sum_{t=0}^{T-1}\frac{\mathbb{E}\|\nabla f(\boldsymbol{x}_t)\|^2}{4\sqrt{G_\infty^2+\epsilon}} \leq \frac{f(\mathbf{0})-f^*}{\gamma T} + \frac{227\gamma^2 L^2 V_1^2(1+\omega)^3 G_\infty^2 d\sqrt{G_\infty^2+\epsilon}(T-m)}{\beta_2^{2m}(1-\beta_1)^2(1-\omega)^4 T} + \frac{L\gamma\sigma^2 V_1(T-m)}{2n\beta_2^m T} + \left(\frac{34}{L}+\frac{1}{4\sqrt{G_\infty^2+\epsilon}}\right)\cdot\left(\frac{\sigma^2}{n}+G_\infty^2 d\right)\frac{m}{T} + \frac{32(1+\beta_1)^2(1+\omega)^3 V_1 G_\infty^2 dmL}{\beta_2^m(1-\beta_1)^2(1-\omega)^4 T}$$

Dropping the constants, we finally obtain

$$\frac{1}{T}\sum_{t=0}^{T-1}\mathbb{E}\|\nabla f(\boldsymbol{x}_t)\|^2 \leq O\left(\frac{f(\mathbf{0})-f^*}{\gamma T} + \frac{\gamma^2}{\beta_2^{2m}(1-\beta_1)^2(1-\omega)^4} + \frac{\gamma\sigma^2}{n\beta_2^m} + \frac{\omega m}{\beta_2^m(1-\beta_1)^2(1-\omega)^4 T} + \frac{\sigma^2 m}{nT}\right).$$

To meet the requirement of learning rate we set

$$\gamma_t = \left(\sigma\sqrt{\frac{T}{n}} + \frac{\beta_2^m}{2V_1 L\sqrt{G_\infty^2+\epsilon}} + \frac{1}{125}\right)^{-1},$$

then it holds that

$$\frac{1}{T}\sum_{t=0}^{T-1}\mathbb{E}\|\nabla f(\boldsymbol{x}_t)\|^2 \leq O\left(\frac{\beta_2^{-m/2}}{\sqrt{nT}} + \frac{(m+n)\beta_2^{-m}}{(1-\omega)^4 T} + \frac{1}{T}\right).$$

That completes the proof. □

D.2. Proof to Theorem 2

Note that the following proof will use Algorithm 3 to replace **1bit-AllReduce** in Algorithm 2, as introduced in Section A.

Proof. We now prove Theorem 2. Similar to the proof to Theorem 1, in this proof we discuss the case of $t \in \mathcal{T}_{\boldsymbol{v}}$ and $t \notin \mathcal{T}_{\boldsymbol{v}}$ separately. Following the proof of Theorem 1, we define the following auxiliary sequence

$$\tilde{\boldsymbol{y}}_t = \tilde{\boldsymbol{x}}_t - \frac{\gamma\tilde{\boldsymbol{m}}_t}{(1-\beta_1)\sqrt{\boldsymbol{v}_t+\epsilon}} - \frac{\gamma\boldsymbol{\delta}_t}{\sqrt{\boldsymbol{v}_t+\epsilon}},$$

where

$$\tilde{\boldsymbol{x}}_t = \frac{1}{n}\sum_{i=1}^n \boldsymbol{x}_t^{(i)}$$
$$\tilde{\boldsymbol{m}}_t = \frac{1}{n}\sum_{i=1}^n \boldsymbol{m}_t^{(i)}.$$

And we additionally define that

$$\tilde{\boldsymbol{u}}_t = \frac{1}{n}\sum_{i=1}^n \boldsymbol{u}_t^{(i)}$$
$$\tilde{\boldsymbol{g}}_t = \frac{1}{n}\sum_{i=1}^n \boldsymbol{g}_t^{(i)}.$$

Note that the definition of $\tilde{\boldsymbol{g}}_t$ is different from the $\boldsymbol{g}_t$ in Theorem 1 since the former is computed on local models which potentially can be different before the sync step.

To expect a compression error bound to scale in the order of $O(\gamma^2)$, we slightly modify the update of line 5, 8, 9 of Algorithm 2 into

$$\boldsymbol{u}_{t+\frac{1}{2}}^{(i)} = \boldsymbol{u}_t^{(i)} + \boldsymbol{m}_t^{(i)}$$

$$\begin{aligned}\boldsymbol{m}_{t+1}^{(i)} =& \overline{\boldsymbol{u}}_{t+\frac{1}{2}} / \sum_{k=t'}^{t}\\ \boldsymbol{x}_{t+1}^{(i)} =& \boldsymbol{x}_{t'}^{(i)} - \gamma \overline{\boldsymbol{u}}_{t+\frac{1}{2}} / \sqrt{\boldsymbol{v}_t + \epsilon}.\end{aligned}$$

Note that since Theorem 2 states the convergence results for constant learning rate, such modification does not change the semantics of the original Algorithm 2. Based on Algorithm 3, we know that

$$\begin{aligned}\overline{\boldsymbol{u}}_{t+\frac{1}{2}} =& \frac{1}{n}\sum_{i=1}^{n} \hat{\boldsymbol{u}}_{t+\frac{1}{2}}^{(i)} + \overline{\boldsymbol{\delta}}_t - \overline{\boldsymbol{\delta}}_{t+1}\\ =& \frac{1}{n}\sum_{i=1}^{n} \left(\boldsymbol{u}_{t+\frac{1}{2}}^{(i)} + \boldsymbol{\delta}_t^{(i)} - \boldsymbol{\delta}_{t+1}^{(i)}\right) + \overline{\boldsymbol{\delta}}_t - \overline{\boldsymbol{\delta}}_{t+1}\\ =& \frac{1}{n}\sum_{i=1}^{n} \boldsymbol{u}_{t+\frac{1}{2}}^{(i)} + \left(\frac{1}{n}\sum_{i=1}^{n} \boldsymbol{\delta}_t^{(i)} - \overline{\boldsymbol{\delta}}_t\right) - \left(\frac{1}{n}\sum_{i=1}^{n} \boldsymbol{\delta}_{t+1}^{(i)} - \overline{\boldsymbol{\delta}}_{t+1}\right)\\ =& \tilde{\boldsymbol{u}}_{t+\frac{1}{2}} + \boldsymbol{\delta}_t - \boldsymbol{\delta}_{t+1}.\end{aligned}$$

Based on Lemma 10, we know that for all the $t \in \mathcal{T}_{\boldsymbol{v}}$, we have the following bound,

$$\sum_{t\in\mathcal{T}_{\boldsymbol{v}}} \frac{\gamma\mathbb{E}\|\nabla f(\tilde{\boldsymbol{x}}_t)\|^2}{4\sqrt{G_\infty^2+\epsilon}} \le \sum_{t\in\mathcal{T}_{\boldsymbol{v}}} \mathbb{E}f(\tilde{\boldsymbol{y}}_t) - \mathbb{E}f(\tilde{\boldsymbol{y}}_{t+1}) + \frac{2\gamma\sigma^2 m}{nL} + \frac{106\gamma H^2 V_1 (M+\Delta^2) mL}{\beta_2^m (1-\beta_1)^2} + \frac{\gamma\sigma^2 m}{4n\sqrt{G_\infty^2+\epsilon}} + \frac{\gamma G_\infty^2 dm}{4\sqrt{G_\infty^2+\epsilon}}.$$

On the other hand, for all the $t \notin \mathcal{T}_{\boldsymbol{v}}$, we have the following bound,

$$\begin{aligned}&\sum_{t\notin\mathcal{T}_{\boldsymbol{v}}} \frac{\gamma\mathbb{E}\left\|\nabla f(\tilde{\boldsymbol{x}}_t)\right\|^2}{4\sqrt{G_\infty^2+\epsilon}}\\ \le& \sum_{t\notin\mathcal{T}_{\boldsymbol{v}}} \mathbb{E}f(\tilde{\boldsymbol{y}}_t) - \mathbb{E}f(\tilde{\boldsymbol{y}}_{t+1}) + \frac{36\gamma^3 H^2 V_1 (3G_\infty^2 d + 25\Delta^2) L^2 (1+L)(G_\infty^2+\epsilon+1)(T-m)}{\beta_2^m (1-\beta_1)^4 \sqrt{G_\infty^2+\epsilon}} + \frac{L\gamma^2 V_1 \sigma^2 (T-m)}{n\beta_2^m}\\ &+ \frac{48\gamma^3 V_1 (H+1)^2 (3G_\infty^2 d + 24\Delta^2)\sqrt{G_\infty^2+\epsilon}(T-m)}{\beta_2^m (1-\beta_1)^4}.\end{aligned}$$

Note that they hold if learning rate is set to be

$$\gamma \le \min\left\{\frac{\beta_2^m}{4V_1 L\sqrt{G_\infty^2+\epsilon}}, \frac{2\sqrt{G_\infty^2+\epsilon}}{L}, \frac{1}{6}\right\}.$$

Combine them together, we obtain

$$\begin{aligned}&\frac{1}{T}\sum_{t=0}^{T-1} \frac{\mathbb{E}\|\nabla f(\boldsymbol{x}_t)\|^2}{4\sqrt{G_\infty^2+\epsilon}}\\ \le& \frac{f(\mathbf{0}) - f^*}{\gamma T} + \frac{2\sigma^2 m}{nLT} + \frac{106 H^2 V_1 (M+\Delta^2) mL}{\beta_2^m (1-\beta_1)^2 T} + \frac{\sigma^2 m}{4n\sqrt{G_\infty^2+\epsilon}T} + \frac{G_\infty^2 dm}{4\sqrt{G_\infty^2+\epsilon}T} + \frac{L\gamma V_1 \sigma^2}{n\beta_2^m}\\ &+ \frac{36\gamma^2 H^2 V_1 (3G_\infty^2 d + 25\Delta^2) L^2 (1+L)(G_\infty^2+\epsilon+1)}{\beta_2^m (1-\beta_1)^4 \sqrt{G_\infty^2+\epsilon}} + \frac{48\gamma^2 V_1 (H+1)^2 (3G_\infty^2 d + 24\Delta^2)\sqrt{G_\infty^2+\epsilon}}{\beta_2^m (1-\beta_1)^4}.\end{aligned}$$

Omitting constants:

$$\frac{1}{T}\sum_{t=0}^{T-1} \mathbb{E}\left\|\nabla f(\tilde{\boldsymbol{x}}_t)\right\|^2 \le O\left(\frac{f(\mathbf{0}) - f^*}{\gamma T} + \frac{\gamma^2 H^2 \Delta^2}{\beta_2^m} + \frac{\gamma\sigma^2}{n\beta_2^m} + \frac{\sigma^2 m}{nT} + \frac{H^2\Delta^2 m}{\beta_2^m T} + \frac{m}{T}\right).$$

If we set

$$\gamma_t = \left(\sigma\sqrt{\frac{T}{n}} + \frac{\beta_2^m}{4V_1 L\sqrt{G_\infty^2+\epsilon}} + \frac{2\sqrt{G_\infty^2+\epsilon}}{L} + \frac{1}{6}\right)^{-1},$$

then it holds that

$$\frac{1}{T}\sum_{t=0}^{T-1}\mathbb{E}\|\nabla f(\boldsymbol{x}_t)\|^2 \le O\left(\frac{\beta_2^{-m/2}}{\sqrt{nT}} + \frac{H^2\Delta^2(m+n)}{\beta_2^m T} + \frac{1}{T}\right).$$

And that completes the proof. □

D.3. Technical Lemma

Lemma 1. *Consider running Algorithm 3 over a communication buffer $\boldsymbol{z}$ (same notation in Algorithm 3) under Assumption 3, let $\boldsymbol{\delta}_t$ denote:*

$$\boldsymbol{\delta}_t = \frac{1}{n}\sum_{i=1}^n \boldsymbol{\delta}_t^{(i)} - \overline{\boldsymbol{\delta}}_t$$

then based on Assumption 3 and 4, it holds that $t \ge 0$, if $\mathbb{E}\|\boldsymbol{z}_t^{(i)}\|^2 \le C$ for some constant $C > 0$,

$$\mathbb{E}\left\|\boldsymbol{\delta}_t\right\|^2 \le \frac{32\omega(1+\omega)^3 C}{(1-\omega)^4}.$$

Proof. Note that the error is initialized by $\mathbf{0}$, so that when $t = 0$ the bound trivially holds. We next prove the case for $t \ge 1$. For any $i \in \{1, \cdots, n\}$ and $t \ge 1$, by the definition of the sequence $\boldsymbol{\delta}_t^{(i)}$,

$$\begin{aligned}
\mathbb{E}\left\|\boldsymbol{\delta}_t^{(i)}\right\|^2 =& \mathbb{E}\left\|\boldsymbol{z}_{t-1}^{(i)} + \boldsymbol{\delta}_{t-1}^{(i)} - \hat{\boldsymbol{z}}_{t-1}^{(i)}\right\|^2 \\
=& \mathbb{E}\left\|\boldsymbol{z}_{t-1}^{(i)} + \boldsymbol{\delta}_{t-1}^{(i)} - \mathcal{C}\left[\boldsymbol{z}_{t-1}^{(i)} + \boldsymbol{\delta}_{t-1}^{(i)}\right]\right\|^2 \\
\overset{\text{Assumption 3}}{\le}& \omega\mathbb{E}\left\|\boldsymbol{z}_{t-1}^{(i)} + \boldsymbol{\delta}_{t-1}^{(i)}\right\|^2 \\
\overset{\forall\eta>0}{\le}& \omega(1+\eta)\mathbb{E}\left\|\boldsymbol{\delta}_{t-1}^{(i)}\right\|^2 + \omega(1+1/\eta)\mathbb{E}\left\|\boldsymbol{z}_{t-1}^{(i)}\right\|^2 \\
\overset{\text{Assumption 4}}{\le}& \sum_{j=0}^{\infty}\left[\omega(1+\eta)\right]^j \omega(1+1/\eta)C \\
\le& \frac{\omega(1+1/\eta)}{1-\omega(1+\eta)}C.
\end{aligned}$$

Selecting $\eta = \frac{1-\omega}{2\omega}$, we obtain

$$\mathbb{E}\left\|\boldsymbol{\delta}_t^{(i)}\right\|^2 \le \frac{2\omega(1+\omega)}{(1-\omega)^2}C.$$

Similarly, we can show that for any $t \ge 1$,

$$\begin{aligned}
\mathbb{E}\left\|\overline{\boldsymbol{\delta}}_t\right\|^2 =& \mathbb{E}\left\|\frac{1}{n}\sum_{i=1}^n \hat{\boldsymbol{z}}_{t-1}^{(i)} + \overline{\boldsymbol{\delta}}_{t-1} - \overline{\boldsymbol{z}}_{t-1}\right\|^2 \\
=& \mathbb{E}\left\|\frac{1}{n}\sum_{i=1}^n \hat{\boldsymbol{z}}_{t-1}^{(i)} + \overline{\boldsymbol{\delta}}_{t-1} - \mathcal{C}\left[\frac{1}{n}\sum_{i=1}^n \hat{\boldsymbol{z}}_{t-1}^{(i)} + \overline{\boldsymbol{\delta}}_{t-1}\right]\right\|^2
\end{aligned}$$

$$
\begin{aligned}
\leq & \omega \mathbb{E}\left\|\frac{1}{n}\sum_{i=1}^{n}\hat{\boldsymbol{z}}_{t-1}^{(i)}+\overline{\boldsymbol{\delta}}_{t-1}\right\|^2 \\
\leq & \omega(1+\eta)\mathbb{E}\left\|\overline{\boldsymbol{\delta}}_{t-1}\right\|^2+\omega(1+1/\eta)\mathbb{E}\left\|\frac{1}{n}\sum_{i=1}^{n}\hat{\boldsymbol{z}}_{t-1}^{(i)}\right\|^2 \\
\leq & \omega(1+\eta)\mathbb{E}\left\|\overline{\boldsymbol{\delta}}_{t-1}\right\|^2+\omega(1+1/\eta)\cdot\frac{1}{n}\sum_{i=1}^{n}\mathbb{E}\left\|\hat{\boldsymbol{z}}_{t-1}^{(i)}\right\|^2,
\end{aligned}
$$

where in the last step we apply the Jensen Inequality. Since we do not assume a bound on the $\left\|\hat{\boldsymbol{z}}_{t-1}^{(i)}\right\|^2$, we need to bound it in terms of

$$
\begin{aligned}
\mathbb{E}\left\|\hat{\boldsymbol{z}}_{t-1}^{(i)}\right\|^2 = & \mathbb{E}\left\|\boldsymbol{z}_{t-1}^{(i)}+\boldsymbol{\delta}_{t-1}^{(i)}-\boldsymbol{\delta}_{t}^{(i)}\right\|^2 \\
\leq & 2\mathbb{E}\left\|\boldsymbol{z}_{t-1}^{(i)}+\boldsymbol{\delta}_{t-1}^{(i)}\right\|^2+2\mathbb{E}\left\|\boldsymbol{\delta}_{t}^{(i)}\right\|^2 \\
\leq & \frac{4(1+\omega)}{(1-\omega)^2}C+\frac{4\omega(1+\omega)}{(1-\omega)^2}C \\
\leq & \frac{4(1+\omega)^2}{(1-\omega)^2}C,
\end{aligned}
$$

where we apply the results from the bound on $\mathbb{E}\left\|\boldsymbol{\delta}_{t}^{(i)}\right\|^2$. Given this bound, and following the analysis for $\mathbb{E}\left\|\boldsymbol{\delta}_{t}^{(i)}\right\|^2$, we can now bound the $\mathbb{E}\left\|\overline{\boldsymbol{\delta}}_{t}\right\|^2$ as follows

$$
\begin{aligned}
\mathbb{E}\left\|\overline{\boldsymbol{\delta}}_{t}\right\|^2 \leq & \frac{2\omega(1+\omega)}{(1-\omega)^2}\cdot\frac{4(1+\omega)^2}{(1-\omega)^2}C \\
= & \frac{8\omega(1+\omega)^3}{(1-\omega)^4}C.
\end{aligned}
$$

Finally, we obtain $t \geq 1$,

$$
\begin{aligned}
\mathbb{E}\left\|\boldsymbol{\delta}_{t}\right\|^2 = & \mathbb{E}\left\|\frac{1}{n}\sum_{i=1}^{n}\boldsymbol{\delta}_{t}^{(i)}-\overline{\boldsymbol{\delta}}_{t}\right\|^2 \\
\leq & 2\mathbb{E}\left\|\overline{\boldsymbol{\delta}}_{t}\right\|^2+2\mathbb{E}\left\|\frac{1}{n}\sum_{i=1}^{n}\boldsymbol{\delta}_{t}^{(i)}\right\|^2 \\
\leq & 2\mathbb{E}\left\|\overline{\boldsymbol{\delta}}_{t}\right\|^2+2\frac{1}{n}\sum_{i=1}^{n}\mathbb{E}\left\|\boldsymbol{\delta}_{t}^{(i)}\right\|^2 \\
\leq & \frac{32\omega(1+\omega)^3C}{(1-\omega)^4}.
\end{aligned}
$$

That completes the proof. □

Lemma 2. *For the variance term, we have the following upper and lower bound: for any $t \geq 1$,*

$$
\beta_2^{m/2}\sqrt{\boldsymbol{v}_1+\epsilon} \leq \sqrt{\boldsymbol{v}_t+\epsilon} \leq \sqrt{G_\infty^2+\epsilon},
$$

where the inequality holds element-wise.

Proof. On one hand, for any $t_j \leq t < t_{j+1}$, where t_j denotes an update step, we obtain element-wise:

$$
\boldsymbol{v}_t \geq \beta_2 \boldsymbol{v}_{t_j} \geq \cdots \geq \beta_2^j \boldsymbol{v}_1 \geq \beta_2^m \boldsymbol{v}_1,
$$

so that

$$\sqrt{\boldsymbol{v}_t+\epsilon} \geq \sqrt{\beta_2^m \boldsymbol{v}_1+\epsilon} \geq \sqrt{\beta_2^m(\boldsymbol{v}_1+\epsilon)} = \beta_2^{m/2}\sqrt{\boldsymbol{v}_1+\epsilon}.$$

On the other hand, for any $t \geq 1$ and $j \in \{1, \cdots, d\}$,

$$[\boldsymbol{v}_t]_j = \sum_{k=1}^{t}(1-\beta_2)\beta_2^{t-k}\left(\frac{1}{n}\sum_{i=1}^{n}[\boldsymbol{g}_k^{(i)}]_j\right)^2 \leq G_\infty^2(1-\beta_2)\sum_{k=1}^{\infty}\beta_2^k \leq G_\infty^2,$$

so that

$$\sqrt{\boldsymbol{v}_t+\epsilon} \leq \sqrt{G_\infty^2+\epsilon}.$$

That completes the proof. □

Lemma 3. *In Algorithm 1, for any $t \geq 0$,*

$$\mathbb{E}\left\|\boldsymbol{m}_t\right\|^2 \leq \frac{195(1+\omega)^3 G_\infty^2 d}{(1-\omega)^4}.$$

Proof. For any $t \geq 0$,

$$\begin{aligned}
\mathbb{E}\left\|\boldsymbol{m}_t\right\|^2 =& \mathbb{E}\left\|(1-\beta_1)\sum_{k=0}^{t}\beta_1^{t-k}\overline{\boldsymbol{g}}_k\right\|^2 \\
\leq& (1-\beta_1)\sum_{k=0}^{t}\beta_1^{t-k}\mathbb{E}\left\|\overline{\boldsymbol{g}}_k\right\|^2 \\
\leq& (1-\beta_1)\sum_{k=0}^{t}\beta_1^{t-k}\mathbb{E}\left\|\boldsymbol{g}_k+\boldsymbol{\delta}_k-\boldsymbol{\delta}_{k+1}\right\|^2 \\
\leq& (1-\beta_1)\sum_{k=0}^{t}\beta_1^{t-k}\left(3\mathbb{E}\left\|\boldsymbol{g}_k\right\|^2+3\mathbb{E}\left\|\boldsymbol{\delta}_k\right\|^2+3\mathbb{E}\left\|\boldsymbol{\delta}_{k+1}\right\|^2\right) \\
\leq& (1-\beta_1)\sum_{k=0}^{t}\beta_1^{t-k}\left(3\mathbb{E}\left\|\frac{1}{n}\sum_{i=1}^{n}\boldsymbol{g}_k^{(i)}\right\|^2+3\mathbb{E}\left\|\boldsymbol{\delta}_k\right\|^2+3\mathbb{E}\left\|\boldsymbol{\delta}_{k+1}\right\|^2\right) \\
\leq& (1-\beta_1)\sum_{k=0}^{t}\beta_1^{t-k}\left(\frac{3}{n}\sum_{i=1}^{n}\mathbb{E}\left\|\boldsymbol{g}_k^{(i)}\right\|^2+3\mathbb{E}\left\|\boldsymbol{\delta}_k\right\|^2+3\mathbb{E}\left\|\boldsymbol{\delta}_{k+1}\right\|^2\right) \\
\overset{(i)}{\leq}& (1-\beta_1)\sum_{k=0}^{t}\beta_1^{t-k}\left(3G_\infty^2 d+\frac{192\omega(1+\omega)^3 G_\infty^2 d}{(1-\omega)^4}\right) \\
\leq& \left(\frac{3(1+\omega)^3 G_\infty^2 d}{(1-\omega)^4}+\frac{192(1+\omega)^3 G_\infty^2 d}{(1-\omega)^4}\right)\cdot(1-\beta_1)\sum_{k=0}^{\infty}\beta_1^k \\
\leq& \frac{195(1+\omega)^3 G_\infty^2 d}{(1-\omega)^4},
\end{aligned}$$

where in the step (i) we use Lemma 1. That completes the proof. □

Lemma 4. *For any $\boldsymbol{a}$, $\boldsymbol{b} \in \mathbb{R}^d$, the following bound holds:*

$$\left\|\frac{\boldsymbol{a}}{\sqrt{\boldsymbol{b}}}\right\|^2 \leq \left\|\boldsymbol{a}\right\|^2\left\|\frac{1}{\boldsymbol{b}}\right\|_1.$$

Proof. Denote the subscript j as the index of the coordinate.

$$\left\|\frac{\boldsymbol{a}}{\sqrt{\boldsymbol{b}}}\right\|^2=\sum_{j=1}^{d}\left(\frac{\boldsymbol{a}_j}{[\sqrt{\boldsymbol{b}}]_j}\right)^2\leq\left(\sum_{j=1}^{d}\boldsymbol{a}_j^2\right)\left(\sum_{j=1}^{d}\frac{1}{\boldsymbol{b}_j}\right)=\left(\sum_{j=1}^{d}\boldsymbol{a}_j^2\right)\left(\sum_{j=1}^{d}\left|\frac{1}{\boldsymbol{b}_j}\right|\right)=\|\boldsymbol{a}\|^2\left\|\frac{1}{\boldsymbol{b}}\right\|_1.$$

Note that the second step holds not because Cauchy-Schwarz Inequality but due to the fact that $\boldsymbol{a}_j^2, \boldsymbol{b}_j > 0$ (since $\sqrt{\boldsymbol{b}}$ would implicitly assume so). □

Lemma 5. *In Algorithm 1, for all the $t \geq 1$ that fulfills $\boldsymbol{v}_t = \boldsymbol{v}_{t+1}$, i.e., $\forall t$ such that $t \notin \mathcal{T}_{\boldsymbol{v}}$, if we let*

$$\gamma\leq\frac{\beta_2^m}{2V_1L\sqrt{G_\infty^2+\epsilon}},$$

the following bound holds,

$$\begin{aligned}&\sum_{t\notin\mathcal{T}_{\boldsymbol{v}}}\frac{\gamma}{4\sqrt{G_\infty^2+\epsilon}}\mathbb{E}\|\nabla f(\boldsymbol{x}_t)\|^2\\&\leq\sum_{t\notin\mathcal{T}_{\boldsymbol{v}}}\mathbb{E}[f(\boldsymbol{y}_t)-f(\boldsymbol{y}_{t+1})]+\frac{227\gamma^3L^2V_1^2(1+\omega)^3G_\infty^2d\sqrt{G_\infty^2+\epsilon}(T-m)}{\beta_2^{2m}(1-\beta_1)^2(1-\omega)^4}+\frac{L\gamma^2\sigma^2V_1(T-m)}{2n\beta_2^m}.\end{aligned}$$

Proof. Recall the auxiliary sequence

$$\boldsymbol{y}_t=\boldsymbol{x}_t-\frac{\gamma\boldsymbol{m}_t}{(1-\beta_1)\sqrt{\boldsymbol{v}_t+\epsilon}}-\frac{\gamma\boldsymbol{\delta}_t}{\sqrt{\boldsymbol{v}_t+\epsilon}},$$

For all the steps $t \geq 0$ that fulfills $\boldsymbol{v}_{t+1} = \boldsymbol{v}_t$, we obtain

$$\begin{aligned}\boldsymbol{y}_{t+1}-\boldsymbol{y}_t=&\boldsymbol{x}_{t+1}-\boldsymbol{x}_t-\frac{\gamma}{1-\beta_1}\left(\frac{\boldsymbol{m}_{t+1}}{\sqrt{\boldsymbol{v}_{t+1}+\epsilon}}-\frac{\boldsymbol{m}_t}{\sqrt{\boldsymbol{v}_t+\epsilon}}\right)-\gamma\left(\frac{\boldsymbol{\delta}_{t+1}}{\sqrt{\boldsymbol{v}_{t+1}+\epsilon}}-\frac{\boldsymbol{\delta}_t}{\sqrt{\boldsymbol{v}_t+\epsilon}}\right)\\=&-\gamma\frac{\boldsymbol{m}_t}{\sqrt{\boldsymbol{v}_t+\epsilon}}-\frac{\gamma}{(1-\beta_1)\sqrt{\boldsymbol{v}_t+\epsilon}}\left(\beta_1\boldsymbol{m}_t+(1-\beta_1)\overline{\boldsymbol{g}}_t-\boldsymbol{m}_t-(1-\beta_1)(\boldsymbol{\delta}_t-\boldsymbol{\delta}_{t+1})\right)\\=&-\frac{\gamma\boldsymbol{g}_t}{\sqrt{\boldsymbol{v}_t+\epsilon}}.\end{aligned}$$

From Assumption 1, we have

$$\begin{aligned}\mathbb{E}f(\boldsymbol{y}_{t+1})-\mathbb{E}f(\boldsymbol{y}_t)\leq&\mathbb{E}\left\langle\nabla f(\boldsymbol{y}_t),\boldsymbol{y}_{t+1}-\boldsymbol{y}_t\right\rangle+\frac{L}{2}\mathbb{E}\left\|\boldsymbol{y}_{t+1}-\boldsymbol{y}_t\right\|^2\\=&-\gamma\mathbb{E}\left\langle\nabla f(\boldsymbol{y}_t),\frac{\boldsymbol{g}_t}{\sqrt{\boldsymbol{v}_t+\epsilon}}\right\rangle+\frac{L\gamma^2}{2}\mathbb{E}\left\|\frac{\boldsymbol{g}_t}{\sqrt{\boldsymbol{v}_t+\epsilon}}\right\|^2\\=&-\gamma\mathbb{E}\left\langle\nabla f(\boldsymbol{y}_t),\frac{\nabla f(\boldsymbol{x}_t)}{\sqrt{\boldsymbol{v}_t+\epsilon}}\right\rangle+\frac{L\gamma^2}{2}\mathbb{E}\left\|\frac{\boldsymbol{g}_t}{\sqrt{\boldsymbol{v}_t+\epsilon}}\right\|^2\\=&-\gamma\mathbb{E}\left\langle\nabla f(\boldsymbol{x}_t),\frac{\nabla f(\boldsymbol{x}_t)}{\sqrt{\boldsymbol{v}_t+\epsilon}}\right\rangle+\gamma\mathbb{E}\left\langle\nabla f(\boldsymbol{x}_t)-\nabla f(\boldsymbol{y}_t),\frac{\nabla f(\boldsymbol{x}_t)}{\sqrt{\boldsymbol{v}_t+\epsilon}}\right\rangle+\frac{L\gamma^2}{2}\mathbb{E}\left\|\frac{\boldsymbol{g}_t}{\sqrt{\boldsymbol{v}_t+\epsilon}}\right\|^2\\=&-\gamma\mathbb{E}\left\langle\nabla f(\boldsymbol{x}_t),\frac{\nabla f(\boldsymbol{x}_t)}{\sqrt{\boldsymbol{v}_t+\epsilon}}\right\rangle+\gamma\mathbb{E}\left\langle\frac{\nabla f(\boldsymbol{x}_t)-\nabla f(\boldsymbol{y}_t)}{\sqrt{\boldsymbol{v}_t+\epsilon}},\nabla f(\boldsymbol{x}_t)\right\rangle+\frac{L\gamma^2}{2}\mathbb{E}\left\|\frac{\boldsymbol{g}_t}{\sqrt{\boldsymbol{v}_t+\epsilon}}\right\|^2\\\leq&-\frac{\gamma\mathbb{E}\left\|\nabla f(\boldsymbol{x}_t)\right\|^2}{\sqrt{G_\infty^2+\epsilon}}+\frac{\gamma}{2\eta}\mathbb{E}\left\|\frac{\nabla f(\boldsymbol{x}_t)-\nabla f(\boldsymbol{y}_t)}{\sqrt{\boldsymbol{v}_t+\epsilon}}\right\|^2+\frac{\gamma\eta}{2}\mathbb{E}\left\|\nabla f(\boldsymbol{x}_t)\right\|^2+\frac{L\gamma^2}{2}\mathbb{E}\left\|\frac{\boldsymbol{g}_t}{\sqrt{\boldsymbol{v}_t+\epsilon}}\right\|^2,\end{aligned}$$

where in the last step we use Lemma 2 and the fact that for any $\boldsymbol{a}, \boldsymbol{b}$ and constant $\eta > 0$,

$$\langle\boldsymbol{a},\boldsymbol{b}\rangle\leq\frac{\eta}{2}\|\boldsymbol{a}\|^2+\frac{1}{2\eta}\|\boldsymbol{b}\|^2.$$

Set $\eta = (\sqrt{G_\infty^2+\epsilon})^{-1}$, with Assumption 1 and Lemma 4,

$$\begin{aligned}
&\mathbb{E}f(\boldsymbol{y}_{t+1}) - \mathbb{E}f(\boldsymbol{y}_t) \\
\leq& -\frac{\gamma\mathbb{E}\left\|\nabla f(\boldsymbol{x}_t)\right\|^2}{2\sqrt{G_\infty^2+\epsilon}} + \frac{\gamma L^2 V_1\sqrt{G_\infty^2+\epsilon}}{2\beta_2^m}\mathbb{E}\left\|\boldsymbol{x}_t-\boldsymbol{y}_t\right\|^2 + \frac{L\gamma^2}{2}\mathbb{E}\left\|\frac{\boldsymbol{g}_t}{\sqrt{\boldsymbol{v}_t+\epsilon}}\right\|^2 \\
=& -\frac{\gamma\mathbb{E}\left\|\nabla f(\boldsymbol{x}_t)\right\|^2}{2\sqrt{G_\infty^2+\epsilon}} + \frac{\gamma L^2 V_1\sqrt{G_\infty^2+\epsilon}}{2\beta_2^m}\mathbb{E}\left\|\frac{\gamma\boldsymbol{m}_t}{(1-\beta_1)\sqrt{\boldsymbol{v}_t+\epsilon}} + \frac{\gamma\boldsymbol{\delta}_t}{\sqrt{\boldsymbol{v}_t+\epsilon}}\right\|^2 + \frac{L\gamma^2}{2}\mathbb{E}\left\|\frac{\boldsymbol{g}_t}{\sqrt{\boldsymbol{v}_t+\epsilon}}\right\|^2 \\
\leq& -\frac{\gamma\mathbb{E}\left\|\nabla f(\boldsymbol{x}_t)\right\|^2}{2\sqrt{G_\infty^2+\epsilon}} + \frac{\gamma^3 L^2 V_1\sqrt{G_\infty^2+\epsilon}}{\beta_2^m(1-\beta_1)^2}\mathbb{E}\left\|\frac{\boldsymbol{m}_t}{\sqrt{\boldsymbol{v}_t+\epsilon}}\right\|^2 + \frac{\gamma^3 L^2 V_1\sqrt{G_\infty^2+\epsilon}}{\beta_2^m}\mathbb{E}\left\|\frac{\boldsymbol{\delta}_t}{\sqrt{\boldsymbol{v}_t+\epsilon}}\right\|^2 + \frac{L\gamma^2}{2}\mathbb{E}\left\|\frac{\boldsymbol{g}_t}{\sqrt{\boldsymbol{v}_t+\epsilon}}\right\|^2 \\
\leq& -\frac{\gamma\mathbb{E}\left\|\nabla f(\boldsymbol{x}_t)\right\|^2}{2\sqrt{G_\infty^2+\epsilon}} + \frac{\gamma^3 L^2 V_1^2\sqrt{G_\infty^2+\epsilon}}{\beta_2^{2m}(1-\beta_1)^2}\mathbb{E}\left\|\boldsymbol{m}_t\right\|^2 + \frac{\gamma^3 L^2 V_1^2\sqrt{G_\infty^2+\epsilon}}{\beta_2^{2m}}\mathbb{E}\left\|\boldsymbol{\delta}_t\right\|^2 + \frac{L\gamma^2 V_1}{2\beta_2^m}\mathbb{E}\left\|\boldsymbol{g}_t\right\|^2,
\end{aligned}$$

where in the last step we apply Lemma 2 and 4. Using the bound on the error from Lemma 1, Lemma 3 and the assumption on the stochastic gradient, we obtain

$$\begin{aligned}
&\left(\frac{\gamma}{2\sqrt{G_\infty^2+\epsilon}} - \frac{L\gamma^2 V_1}{2\beta_2^m}\right)\mathbb{E}\left\|\nabla f(\boldsymbol{x}_t)\right\|^2 \\
\leq& \mathbb{E}[f(\boldsymbol{y}_t) - f(\boldsymbol{y}_{t+1})] + \frac{\gamma^3 L^2 V_1^2\sqrt{G_\infty^2+\epsilon}}{\beta_2^{2m}(1-\beta_1)^2}\mathbb{E}\left\|\boldsymbol{m}_t\right\|^2 + \frac{\gamma^3 L^2 V_1^2\sqrt{G_\infty^2+\epsilon}}{\beta_2^{2m}}\mathbb{E}\left\|\boldsymbol{\delta}_t\right\|^2 + \frac{L\gamma^2\sigma^2 V_1}{2n\beta_2^m} \\
\leq& \mathbb{E}[f(\boldsymbol{y}_t) - f(\boldsymbol{y}_{t+1})] + \frac{195\gamma^3 L^2 V_1^2(1+\omega)^3 G_\infty^2 d\sqrt{G_\infty^2+\epsilon}}{\beta_2^{2m}(1-\beta_1)^2(1-\omega)^4} + \frac{32\gamma^3 L^2 V_1^2\omega(1+\omega)^3 G_\infty^2 d\sqrt{G_\infty^2+\epsilon}}{\beta_2^{2m}(1-\omega)^4} + \frac{L\gamma^2\sigma^2 V_1}{2n\beta_2^m} \\
\leq& \mathbb{E}[f(\boldsymbol{y}_t) - f(\boldsymbol{y}_{t+1})] + \frac{227\gamma^3 L^2 V_1^2(1+\omega)^3 G_\infty^2 d\sqrt{G_\infty^2+\epsilon}}{\beta_2^{2m}(1-\beta_1)^2(1-\omega)^4} + \frac{L\gamma^2\sigma^2 V_1}{2n\beta_2^m}.
\end{aligned}$$

Based on the learning rate bound

$$\gamma \leq \frac{\beta_2^m}{2V_1 L\sqrt{G_\infty^2+\epsilon}},$$

and summing over all the reuse steps, we obtain

$$\begin{aligned}
&\sum_{t\notin\mathcal{T}_{\boldsymbol{v}}}\frac{\gamma}{4\sqrt{G_\infty^2+\epsilon}}\mathbb{E}\|\nabla f(\boldsymbol{x}_t)\|^2 \\
\leq& \sum_{t\notin\mathcal{T}_{\boldsymbol{v}}}\mathbb{E}[f(\boldsymbol{y}_t) - f(\boldsymbol{y}_{t+1})] + \frac{227\gamma^3 L^2 V_1^2(1+\omega)^3 G_\infty^2 d\sqrt{G_\infty^2+\epsilon}(T-m)}{\beta_2^{2m}(1-\beta_1)^2(1-\omega)^4} + \frac{L\gamma^2\sigma^2 V_1(T-m)}{2n\beta_2^m}.
\end{aligned}$$

That completes the proof. □

Lemma 6. *In Algorithm 1, for all the $t \geq 0$ that fulfills $\boldsymbol{v}_t \neq \boldsymbol{v}_{t+1}$, i.e. $t \in \mathcal{T}_{\boldsymbol{v}}$, if the learning rate fulfills*

$$\gamma < \frac{1}{125}$$

, the following bound holds

$$\begin{aligned}
\sum_{t\in\mathcal{T}_{\boldsymbol{v}}}\frac{\gamma}{4\sqrt{G_\infty^2+\epsilon}}\mathbb{E}\|\nabla f(\boldsymbol{x}_t)\|^2 \leq& \sum_{t\in\mathcal{T}_{\boldsymbol{v}}}\mathbb{E}[f(\boldsymbol{y}_t) - f(\boldsymbol{y}_{t+1})] + \left(\frac{34\gamma}{L} + \frac{\gamma}{4\sqrt{G_\infty^2+\epsilon}}\right)\cdot\left(\frac{\sigma^2}{n} + G_\infty^2 d\right)m \\
&+\frac{32\gamma(1+\beta_1)^2(1+\omega)^3 V_1 G_\infty^2 dmL}{\beta_2^m(1-\beta_1)^2(1-\omega)^4}.
\end{aligned}$$

Proof. For all the steps t that fulfills $\boldsymbol{v}_t \neq \boldsymbol{v}_{t+1}$,

$$\begin{aligned}
\boldsymbol{y}_{t+1} - \boldsymbol{y}_t =& \boldsymbol{x}_{t+1} - \boldsymbol{x}_t - \frac{\gamma}{1-\beta_1}\left(\frac{\boldsymbol{m}_{t+1}}{\sqrt{\boldsymbol{v}_{t+1}+\epsilon}} - \frac{\boldsymbol{m}_t}{\sqrt{\boldsymbol{v}_t+\epsilon}}\right) + \gamma\left(\frac{\boldsymbol{\delta}_t}{\sqrt{\boldsymbol{v}_t+\epsilon}} - \frac{\boldsymbol{\delta}_{t+1}}{\sqrt{\boldsymbol{v}_{t+1}+\epsilon}}\right) \\
=& -\gamma\frac{\boldsymbol{m}_t}{\sqrt{\boldsymbol{v}_t+\epsilon}} - \frac{\gamma}{1-\beta_1}\left(\frac{\boldsymbol{m}_{t+1}}{\sqrt{\boldsymbol{v}_{t+1}+\epsilon}} - \frac{\boldsymbol{m}_t}{\sqrt{\boldsymbol{v}_t+\epsilon}}\right) + \gamma\left(\frac{\boldsymbol{\delta}_t}{\sqrt{\boldsymbol{v}_t+\epsilon}} - \frac{\boldsymbol{\delta}_{t+1}}{\sqrt{\boldsymbol{v}_{t+1}+\epsilon}}\right) \\
=& -\frac{\gamma\beta_1}{1-\beta_1}\frac{\boldsymbol{m}_t}{\sqrt{\boldsymbol{v}_t+\epsilon}} - \frac{\gamma}{1-\beta_1}\frac{\boldsymbol{m}_{t+1}}{\sqrt{\boldsymbol{v}_{t+1}+\epsilon}} + \gamma\left(\frac{\boldsymbol{\delta}_t}{\sqrt{\boldsymbol{v}_t+\epsilon}} - \frac{\boldsymbol{\delta}_{t+1}}{\sqrt{\boldsymbol{v}_{t+1}+\epsilon}}\right).
\end{aligned}$$

Based on the smoothness assumption, for constant $\eta > 0$ that will be assigned later,

$$\begin{aligned}
\mathbb{E}f(\boldsymbol{y}_{t+1}) - \mathbb{E}f(\boldsymbol{y}_t) \leq& \mathbb{E}\left\langle \nabla f(\boldsymbol{y}_t), \boldsymbol{y}_{t+1} - \boldsymbol{y}_t\right\rangle + \frac{L}{2}\mathbb{E}\left\|\boldsymbol{y}_{t+1} - \boldsymbol{y}_t\right\|^2 \\
\overset{\gamma\eta\leq 1}{\leq}& \frac{\eta\gamma}{2L}\mathbb{E}\left\|\nabla f(\boldsymbol{y}_t)\right\|^2 + \frac{L}{\eta\gamma}\mathbb{E}\left\|\boldsymbol{y}_{t+1} - \boldsymbol{y}_t\right\|^2 \\
\leq& \frac{\eta\gamma}{L}\mathbb{E}\left\|\nabla f(\boldsymbol{x}_t)\right\|^2 + \eta\gamma L\mathbb{E}\left\|\boldsymbol{y}_t - \boldsymbol{x}_t\right\|^2 + \frac{L}{\eta\gamma}\mathbb{E}\left\|\boldsymbol{y}_{t+1} - \boldsymbol{y}_t\right\|^2 \\
\leq& \frac{\eta\gamma}{L}\mathbb{E}\left\|\nabla f(\boldsymbol{x}_t) - \boldsymbol{g}_t\right\|^2 + \frac{\eta\gamma}{L}\mathbb{E}\left\|\boldsymbol{g}_t\right\|^2 + \eta\gamma L\mathbb{E}\left\|\boldsymbol{y}_t - \boldsymbol{x}_t\right\|^2 + \frac{L}{\eta\gamma}\mathbb{E}\left\|\boldsymbol{y}_{t+1} - \boldsymbol{y}_t\right\|^2 \\
\leq& \frac{\eta\gamma}{n^2L}\sum_{i=1}^n\mathbb{E}\left\|\nabla f(\boldsymbol{x}_t) - \boldsymbol{g}_t^{(i)}\right\|^2 + \frac{\eta\gamma}{nL}\sum_{i=1}^n\mathbb{E}\left\|\boldsymbol{g}_t^{(i)}\right\|^2 + \eta\gamma L\mathbb{E}\left\|\boldsymbol{y}_t - \boldsymbol{x}_t\right\|^2 + \frac{L}{\eta\gamma}\mathbb{E}\left\|\boldsymbol{y}_{t+1} - \boldsymbol{y}_t\right\|^2 \\
\leq& \frac{\eta\gamma}{L}\left(\frac{\sigma^2}{n} + G_\infty^2 d\right) + \eta\gamma L\mathbb{E}\left\|\boldsymbol{y}_t - \boldsymbol{x}_t\right\|^2 + \frac{L}{\eta\gamma}\mathbb{E}\left\|\boldsymbol{y}_{t+1} - \boldsymbol{y}_t\right\|^2.
\end{aligned}$$

Now we can bound the last two terms as follows, note that

$$\begin{aligned}
\mathbb{E}\left\|\boldsymbol{y}_t - \boldsymbol{x}_t\right\|^2 =& \mathbb{E}\left\|\frac{\gamma\boldsymbol{m}_t}{(1-\beta_1)\sqrt{\boldsymbol{v}_t+\epsilon}} + \frac{\gamma\boldsymbol{\delta}_t}{\sqrt{\boldsymbol{v}_t+\epsilon}}\right\|^2 \\
\leq& \frac{2\gamma^2}{(1-\beta_1)^2}\mathbb{E}\left\|\frac{\boldsymbol{m}_t}{\sqrt{\boldsymbol{v}_t+\epsilon}}\right\|^2 + 2\gamma^2\mathbb{E}\left\|\frac{\boldsymbol{\delta}_t}{\sqrt{\boldsymbol{v}_t+\epsilon}}\right\|^2 \\
\leq& \frac{2\gamma^2 V_1}{(1-\beta_1)^2\beta_2^m}\mathbb{E}\left\|\boldsymbol{m}_t\right\|^2 + \frac{2\gamma^2 V_1}{\beta_2^m}\mathbb{E}\left\|\boldsymbol{\delta}_t\right\|^2 \\
\leq& \frac{390\gamma^2(1+\omega)^3 V_1 G_\infty^2 d}{\beta_2^m(1-\beta_1)^2(1-\omega)^4} + \frac{64\gamma^2\omega(1+\omega)^3 V_1 G_\infty^2 d}{\beta_2^m(1-\omega)^4} \\
\leq& \frac{454\gamma^2(1+\omega)^3 V_1 G_\infty^2 d}{\beta_2^m(1-\beta_1)^2(1-\omega)^4},
\end{aligned}$$

where in the last step we apply Lemma 1. On the other hand,

$$\begin{aligned}
&\mathbb{E}\left\|\boldsymbol{y}_{t+1} - \boldsymbol{y}_t\right\|^2 \\
=& \mathbb{E}\left\|\frac{\gamma\beta_1}{1-\beta_1}\frac{\boldsymbol{m}_t}{\sqrt{\boldsymbol{v}_t+\epsilon}} + \frac{\gamma}{1-\beta_1}\frac{\boldsymbol{m}_{t+1}}{\sqrt{\boldsymbol{v}_{t+1}+\epsilon}} - \gamma\left(\frac{\boldsymbol{\delta}_t}{\sqrt{\boldsymbol{v}_t+\epsilon}} - \frac{\boldsymbol{\delta}_{t+1}}{\sqrt{\boldsymbol{v}_{t+1}+\epsilon}}\right)\right\|^2 \\
\leq& \mathbb{E}\left\|\frac{\gamma\beta_1}{1-\beta_1}\frac{\boldsymbol{m}_t}{\sqrt{\boldsymbol{v}_t+\epsilon}} + \frac{\gamma}{1-\beta_1}\frac{\boldsymbol{m}_{t+1}}{\sqrt{\boldsymbol{v}_{t+1}+\epsilon}} - \gamma\left(\frac{\boldsymbol{\delta}_t}{\sqrt{\boldsymbol{v}_t+\epsilon}} - \frac{\boldsymbol{\delta}_{t+1}}{\sqrt{\boldsymbol{v}_{t+1}+\epsilon}}\right)\right\|^2 \\
\leq& \frac{4\gamma^2\beta_1^2}{(1-\beta_1)^2}\mathbb{E}\left\|\frac{\boldsymbol{m}_t}{\sqrt{\boldsymbol{v}_t+\epsilon}}\right\|^2 + \frac{4\gamma^2}{(1-\beta_1)^2}\mathbb{E}\left\|\frac{\boldsymbol{m}_{t+1}}{\sqrt{\boldsymbol{v}_{t+1}+\epsilon}}\right\|^2 + 4\gamma^2\mathbb{E}\left\|\frac{\boldsymbol{\delta}_t}{\sqrt{\boldsymbol{v}_t+\epsilon}}\right\|^2 + 4\gamma^2\mathbb{E}\left\|\frac{\boldsymbol{\delta}_{t+1}}{\sqrt{\boldsymbol{v}_{t+1}+\epsilon}}\right\|^2 \\
\leq& \frac{4\gamma^2\beta_1^2 V_1}{(1-\beta_1)^2\beta_2^m}\mathbb{E}\left\|\boldsymbol{m}_t\right\|^2 + \frac{4\gamma^2 V_1}{(1-\beta_1)^2\beta_2^m}\mathbb{E}\left\|\boldsymbol{m}_{t+1}\right\|^2 + \frac{4\gamma^2 V_1}{\beta_2^m}\mathbb{E}\left\|\boldsymbol{\delta}_t\right\|^2 + \frac{4\gamma^2 V_1}{\beta_2^m}\mathbb{E}\left\|\boldsymbol{\delta}_{t+1}\right\|^2 \\
\leq& \frac{780\gamma^2(1+\beta_1^2)V_1(1+\omega)^3 G_\infty^2 d}{\beta_2^m(1-\beta_1)^2(1-\omega)^4} + \frac{256\gamma^2 V_1\omega(1+\omega)^3 G_\infty^2 d}{\beta_2^m(1-\omega)^4}
\end{aligned}$$

$$\leq \frac{1036\gamma^2(1+\beta_1^2)V_1(1+\omega)^3G_\infty^2 d}{\beta_2^m(1-\beta_1)^2(1-\omega)^4},$$

where we again apply Lemma 1 and Lemma 3. Put everything together,

$$\begin{aligned}
&\mathbb{E}f(\boldsymbol{y}_{t+1}) - \mathbb{E}f(\boldsymbol{y}_t) \\
\leq &\frac{\eta\gamma}{L}\left(\frac{\sigma^2}{n} + G_\infty^2 d\right) + \eta\gamma L\mathbb{E}\left\|\boldsymbol{y}_t - \boldsymbol{x}_t\right\|^2 + \frac{L}{\eta\gamma}\mathbb{E}\left\|\boldsymbol{y}_{t+1} - \boldsymbol{y}_t\right\|^2 \\
\leq &\frac{\eta\gamma}{L}\left(\frac{\sigma^2}{n} + G_\infty^2 d\right) + \frac{454\eta\gamma^3(1+\omega)^3V_1G_\infty^2 dL}{\beta_2^m(1-\beta_1)^2(1-\omega)^4} + \frac{1036\gamma(1+\beta_1^2)V_1(1+\omega)^3G_\infty^2 dL}{\eta\beta_2^m(1-\beta_1)^2(1-\omega)^4} \\
\leq &\frac{\eta\gamma}{L}\left(\frac{\sigma^2}{n} + G_\infty^2 d\right) + \left(454\eta\gamma^2 + \frac{1036}{\eta}\right)\frac{\gamma(1+\beta_1)^2(1+\omega)^3V_1G_\infty^2 dL}{\beta_2^m(1-\beta_1)^2(1-\omega)^4}
\end{aligned}$$

Set $\eta = 34$, and considering $\gamma < \frac{1}{125}$, we get

$$\mathbb{E}f(\boldsymbol{y}_{t+1}) - \mathbb{E}f(\boldsymbol{y}_t) \leq \frac{34\gamma}{L}\left(\frac{\sigma^2}{n} + G_\infty^2 d\right) + \frac{32\gamma(1+\beta_1)^2(1+\omega)^3V_1G_\infty^2 dL}{\beta_2^m(1-\beta_1)^2(1-\omega)^4}.$$

Summing over all the update steps, we obtain

$$0 \leq \sum_{t\in\mathcal{T}_v}\mathbb{E}[f(\boldsymbol{y}_t) - f(\boldsymbol{y}_{t+1})] + \frac{34\gamma}{L}\left(\frac{\sigma^2 m}{n} + G_\infty^2 dm\right) + \frac{32\gamma(1+\beta_1)^2(1+\omega)^3V_1G_\infty^2 dmL}{\beta_2^m(1-\beta_1)^2(1-\omega)^4}.$$

Adding $\frac{\gamma}{4\sqrt{G_\infty^2+\epsilon}}\sum_{t\in\mathcal{T}_v}\mathbb{E}\|\nabla f(\boldsymbol{x}_t)\|^2$ on both sides, and note that

$$\begin{aligned}
\sum_{t\in\mathcal{T}_v}\mathbb{E}\|\nabla f(\boldsymbol{x}_t)\|^2 &= \sum_{t\in\mathcal{T}_v}\mathbb{E}\left\|\nabla f(\boldsymbol{x}_t) - \boldsymbol{g}_t\right\|^2 + \sum_{t\in\mathcal{T}_v}\mathbb{E}\left\|\boldsymbol{g}_t\right\|^2 \\
&\leq \frac{\sigma^2 m}{n} + G_\infty^2 dm,
\end{aligned}$$

we finally obtain

$$\begin{aligned}
\sum_{t\in\mathcal{T}_v}\frac{\gamma}{4\sqrt{G_\infty^2+\epsilon}}\mathbb{E}\|\nabla f(\boldsymbol{x}_t)\|^2 \leq &\sum_{t\in\mathcal{T}_v}\mathbb{E}[f(\boldsymbol{y}_t) - f(\boldsymbol{y}_{t+1})] + \left(\frac{34\gamma}{L} + \frac{\gamma}{4\sqrt{G_\infty^2+\epsilon}}\right)\cdot\left(\frac{\sigma^2}{n} + G_\infty^2 d\right)m \\
&+ \frac{32\gamma(1+\beta_1)^2(1+\omega)^3V_1G_\infty^2 dmL}{\beta_2^m(1-\beta_1)^2(1-\omega)^4}.
\end{aligned}$$

That completes the proof. □

Lemma 7. *Under Assumption 5, for any $t \geq 0$, it holds that*

$$\mathbb{E}\left\|\boldsymbol{\delta}_t\right\|^2 \leq 4\Delta^2.$$

Proof. Based on the definition of the compression error, we obtain

$$\begin{aligned}
\mathbb{E}\left\|\boldsymbol{\delta}_t\right\|^2 =&\mathbb{E}\left\|\frac{1}{n}\sum_{i=1}^n \boldsymbol{\delta}_t^{(i)} - \overline{\boldsymbol{\delta}}_t\right\|^2 \\
\leq &2\mathbb{E}\left\|\overline{\boldsymbol{\delta}}_t\right\|^2 + 2\mathbb{E}\left\|\frac{1}{n}\sum_{i=1}^n \boldsymbol{\delta}_t^{(i)}\right\|^2 \\
\leq &2\mathbb{E}\left\|\overline{\boldsymbol{\delta}}_t\right\|^2 + 2\frac{1}{n}\sum_{i=1}^n\mathbb{E}\left\|\boldsymbol{\delta}_t^{(i)}\right\|^2 \\
\leq &4\Delta^2.
\end{aligned}$$

That completes the proof. □

Lemma 8. *In Algorithm 2, for any $t \geq 0$, the momentum term is uniformly bounded by the following:*

$$\begin{aligned}
\mathbb{E}\left\|\boldsymbol{m}_t^{(i)}\right\|^2 \leq & \frac{3G_\infty^2 d + 24\Delta^2}{(1-\beta_1)^2}, \\
\mathbb{E}\left\|\boldsymbol{m}_{t+\frac{1}{2}}^{(i)}\right\|^2 \leq & \frac{3G_\infty^2 d + 24\Delta^2}{(1-\beta_1)^2}, \\
\mathbb{E}\left\|\tilde{\boldsymbol{m}}_t\right\|^2 \leq & \frac{3G_\infty^2 d + 24\Delta^2}{(1-\beta_1)^2}, \\
\mathbb{E}\left\|\tilde{\boldsymbol{m}}_{t+\frac{1}{2}}\right\|^2 \leq & \frac{3G_\infty^2 d + 24\Delta^2}{(1-\beta_1)^2}.
\end{aligned}$$

Proof. We prove this lemma via induction. Note that when $t = 0$, the inequality trivially holds due to initialization at $\mathbf{0}$ and Jensen Inequality. Now suppose the inequality holds up to step $t \geq 0$, then for $t+1$,

if $t \in \mathcal{T}_{\boldsymbol{u}}$, then

$$\begin{aligned}
&\mathbb{E}\left\|\boldsymbol{m}_{t+1}^{(i)}\right\|^2 \\
=&\mathbb{E}\left\|\frac{\overline{\boldsymbol{u}}_{t+\frac{1}{2}}}{t-k}\right\|^2 \\
=&\mathbb{E}\left\|\frac{\tilde{\boldsymbol{u}}_{t+\frac{1}{2}} + \boldsymbol{\delta}_t - \boldsymbol{\delta}_{t+1}}{t-k}\right\|^2 \\
=&\mathbb{E}\left\|\frac{\sum_{j=k+1}^{t} \tilde{\boldsymbol{m}}_j + \boldsymbol{\delta}_t - \boldsymbol{\delta}_{t+1}}{t-k}\right\|^2 \\
=&\mathbb{E}\left\|\frac{\sum_{j=k+1}^{t}\left(\beta_1^{j-k}\tilde{\boldsymbol{m}}_k + (1-\beta_1)\sum_{h=k}^{j-1}\beta_1^{j-h-1}\boldsymbol{g}_h\right) + \boldsymbol{\delta}_t - \boldsymbol{\delta}_{t+1}}{t-k}\right\|^2 \\
=&\mathbb{E}\left\|\frac{1}{t-k}\sum_{j=k+1}^{t}\beta_1^{j-k}\tilde{\boldsymbol{m}}_k + \frac{1-\beta_1}{t-k}\sum_{j=k+1}^{t}\sum_{h=k}^{j-1}\beta_1^{j-h-1}\boldsymbol{g}_h + (\boldsymbol{\delta}_t - \boldsymbol{\delta}_{t+1})\right\|^2 \\
\overset{\forall \eta>0}{\leq}& (1+\eta)\mathbb{E}\left\|\frac{1}{t-k}\sum_{j=k+1}^{t}\beta_1^{j-k}\tilde{\boldsymbol{m}}_k\right\|^2 + (1+1/\eta)\mathbb{E}\left\|\frac{1-\beta_1}{t-k}\sum_{j=k+1}^{t}\sum_{h=k}^{j-1}\beta_1^{j-h-1}\boldsymbol{g}_h + (\boldsymbol{\delta}_t - \boldsymbol{\delta}_{t+1})\right\|^2 \\
\leq& \frac{1+\eta}{t-k}\sum_{j=k+1}^{t}\mathbb{E}\left\|\beta_1^{j-k}\tilde{\boldsymbol{m}}_k\right\|^2 + \frac{3(1+1/\eta)(1-\beta_1)}{t-k}\sum_{j=k+1}^{t}\sum_{h=k}^{j-1}\beta_1^{j-h-1}\boldsymbol{g}_h\mathbb{E}\left\|\boldsymbol{g}_h\right\|^2 + 3(1+1/\eta)\mathbb{E}\left\|\boldsymbol{\delta}_t\right\|^2 \\
&+ 3(1+1/\eta)\mathbb{E}\left\|\boldsymbol{\delta}_{t+1}\right\|^2 \\
\overset{\eta=1/\beta_1-1}{\leq}& (1+\eta)\beta_1^2 \cdot \frac{3G_\infty^2 d + 24\Delta^2}{(1-\beta_1)^2} + 3(1+1/\eta)G_\infty^2 d + 24(1+1/\eta)\Delta^2 \\
=&\beta_1 \cdot \frac{3G_\infty^2 d + 24\Delta^2}{(1-\beta_1)^2} + \frac{3G_\infty^2 d + 24\Delta^2}{(1-\beta_1)^2} \\
=&\frac{3G_\infty^2 d + 24\Delta^2}{(1-\beta_1)^2}.
\end{aligned}$$

On the other hand, if $t \notin \mathcal{T}_{\boldsymbol{u}}$, then

$$\mathbb{E}\left\|\boldsymbol{m}_{t+1}^{(i)}\right\|^2 = \mathbb{E}\left\|\boldsymbol{m}_{t+\frac{1}{2}}^{(i)}\right\|^2 = \mathbb{E}\left\|\beta_1\boldsymbol{m}_t^{(i)} + (1-\beta_1)\boldsymbol{g}_t^{(i)}\right\|^2 \leq \beta_1\mathbb{E}\left\|\beta_1\boldsymbol{m}_t^{(i)}\right\|^2 + (1-\beta_1)\mathbb{E}\left\|\boldsymbol{g}_t^{(i)}\right\|^2 \leq \frac{3G_\infty^2 d + 24\Delta^2}{(1-\beta_1)^2}.$$

For all the $t + \frac{1}{2}$ case, the inequality holds trivially due to Jensen Inequality. Finally, all the $\tilde{\cdot}$ bound can also be obtained via Jensen Inequality. And that completes the proof. □

Lemma 9. *In Algorithm 2, for all the t such that $t \notin \mathcal{T}_{\boldsymbol{v}}$, it holds that if we set learning rate*

$$\gamma \leq \min\left\{\frac{\beta_2^m}{4V_1 L\sqrt{G_\infty^2+\epsilon}}, \frac{2\sqrt{G_\infty^2+\epsilon}}{L}\right\},$$

then,

$$\begin{aligned}
&\sum_{t\notin\mathcal{T}_{\boldsymbol{v}}} \frac{\gamma\mathbb{E}\left\|\nabla f(\tilde{\boldsymbol{x}}_t)\right\|^2}{4\sqrt{G_\infty^2+\epsilon}} \\
\leq &\sum_{t\notin\mathcal{T}_{\boldsymbol{v}}} \mathbb{E}f(\tilde{\boldsymbol{y}}_t) - \mathbb{E}f(\tilde{\boldsymbol{y}}_{t+1}) + \frac{36\gamma^3H^2V_1(3G_\infty^2 d+25\Delta^2)L^2(1+L)(G_\infty^2+\epsilon+1)(T-m)}{\beta_2^m(1-\beta_1)^4\sqrt{G_\infty^2+\epsilon}} + \frac{L\gamma^2V_1\sigma^2(T-m)}{n\beta_2^m} \\
&+ \frac{48\gamma^3V_1(H+1)^2(3G_\infty^2 d+24\Delta^2)\sqrt{G_\infty^2+\epsilon}(T-m)}{\beta_2^m(1-\beta_1)^4}.
\end{aligned}$$

Proof. Since when $t \notin \mathcal{T}_{\boldsymbol{v}}$, it can either belongs to $\mathcal{T}_{\boldsymbol{u}}$ or not. We first prove the case for $t \in \mathcal{T}_{\boldsymbol{u}}$. From the definition of the auxiliary sequence, we obtain,

$$\begin{aligned}
\tilde{\boldsymbol{y}}_{t+1} - \tilde{\boldsymbol{y}}_t =&\tilde{\boldsymbol{x}}_{t+1} - \tilde{\boldsymbol{x}}_t - \frac{\gamma}{1-\beta_1}\left(\frac{\tilde{\boldsymbol{m}}_{t+1}}{\sqrt{\boldsymbol{v}_{t+1}+\epsilon}} - \frac{\tilde{\boldsymbol{m}}_t}{\sqrt{\boldsymbol{v}_t+\epsilon}}\right) - \left(\frac{\gamma\boldsymbol{\delta}_{t+1}}{\sqrt{\boldsymbol{v}_{t+1}+\epsilon}} - \frac{\gamma\boldsymbol{\delta}_t}{\sqrt{\boldsymbol{v}_t+\epsilon}}\right) \\
=&\tilde{\boldsymbol{x}}_{t+1} - \tilde{\boldsymbol{x}}_t - \frac{\gamma}{(1-\beta_1)\sqrt{\boldsymbol{v}_t+\epsilon}}\left(\tilde{\boldsymbol{m}}_{t+1} - \tilde{\boldsymbol{m}}_t\right) - \frac{1}{\sqrt{\boldsymbol{v}_t+\epsilon}}(\gamma\boldsymbol{\delta}_{t+1} - \gamma\boldsymbol{\delta}_t) \\
=&\tilde{\boldsymbol{x}}_{t+\frac{1}{2}} - \tilde{\boldsymbol{x}}_t - \frac{\gamma}{(1-\beta_1)\sqrt{\boldsymbol{v}_t+\epsilon}}\left(\tilde{\boldsymbol{m}}_{t+\frac{1}{2}} - \tilde{\boldsymbol{m}}_t\right) \\
&\underbrace{+\tilde{\boldsymbol{x}}_{t+1} - \tilde{\boldsymbol{x}}_{t+\frac{1}{2}} - \frac{\gamma}{(1-\beta_1)\sqrt{\boldsymbol{v}_t+\epsilon}}\left(\tilde{\boldsymbol{m}}_{t+1} - \tilde{\boldsymbol{m}}_{t+\frac{1}{2}}\right) - \frac{1}{\sqrt{\boldsymbol{v}_t+\epsilon}}(\gamma\boldsymbol{\delta}_{t+1} - \gamma\boldsymbol{\delta}_t)}_{=\boldsymbol{q}_t} \\
=&-\frac{\gamma\tilde{\boldsymbol{m}}_t}{\sqrt{\boldsymbol{v}_t+\epsilon}} - \frac{\gamma}{(1-\beta_1)\sqrt{\boldsymbol{v}_t+\epsilon}}\left(\beta_1\tilde{\boldsymbol{m}}_t + (1-\beta_1)\tilde{\boldsymbol{g}}_t - \tilde{\boldsymbol{m}}_t\right) + \boldsymbol{q}_t \\
=&-\frac{\gamma\tilde{\boldsymbol{g}}_t}{\sqrt{\boldsymbol{v}+\epsilon}} + \boldsymbol{q}_t.
\end{aligned}$$

From Assumption 1, we have

$$\begin{aligned}
\mathbb{E}f(\tilde{\boldsymbol{y}}_{t+1}) - \mathbb{E}f(\tilde{\boldsymbol{y}}_t) \leq&\mathbb{E}\left\langle\nabla f(\tilde{\boldsymbol{y}}_t), \tilde{\boldsymbol{y}}_{t+1} - \tilde{\boldsymbol{y}}_t\right\rangle + \frac{L}{2}\mathbb{E}\left\|\tilde{\boldsymbol{y}}_{t+1} - \tilde{\boldsymbol{y}}_t\right\|^2 \\
=&\underbrace{-\gamma\mathbb{E}\left\langle\nabla f(\tilde{\boldsymbol{y}}_t), \frac{\tilde{\boldsymbol{g}}_t}{\sqrt{\boldsymbol{v}_t+\epsilon}}\right\rangle}_{A_1} + \underbrace{L\gamma^2\mathbb{E}\left\|\frac{\tilde{\boldsymbol{g}}_t}{\sqrt{\boldsymbol{v}_t+\epsilon}}\right\|^2}_{A_2} \underbrace{-\gamma\mathbb{E}\left\langle\nabla f(\tilde{\boldsymbol{y}}_t), \boldsymbol{q}_t\right\rangle}_{A_3} + \underbrace{L\gamma^2\mathbb{E}\left\|\boldsymbol{q}_t\right\|^2}_{A_4}.
\end{aligned}$$

We now bound A_1 to A_4 separately. Note that from Lemma 8, the momentum term can be uniformly bounded by a constant. For brevity of the derivation, we use M to denote such constant bound, and fit in its value at the end of the proof.

For A_1,

$$\begin{aligned}
A_1 =& -\gamma\mathbb{E}\left\langle\nabla f(\tilde{\boldsymbol{y}}_t), \frac{\tilde{\boldsymbol{g}}_t}{\sqrt{\boldsymbol{v}_t+\epsilon}}\right\rangle \\
=& -\gamma\mathbb{E}\left\langle\nabla f(\tilde{\boldsymbol{y}}_t), \frac{\frac{1}{n}\sum_{i=1}^n \nabla f\left(\boldsymbol{x}_t^{(i)}\right)}{\sqrt{\boldsymbol{v}_t+\epsilon}}\right\rangle \\
=& -\gamma\mathbb{E}\left\langle\nabla f(\tilde{\boldsymbol{x}}_t), \frac{\nabla f(\tilde{\boldsymbol{x}}_t)}{\sqrt{\boldsymbol{v}_t+\epsilon}}\right\rangle - \gamma\mathbb{E}\left\langle\nabla f(\tilde{\boldsymbol{x}}_t), \frac{\frac{1}{n}\sum_{i=1}^n \nabla f\left(\boldsymbol{x}_t^{(i)}\right) - \nabla f(\tilde{\boldsymbol{x}}_t)}{\sqrt{\boldsymbol{v}_t+\epsilon}}\right\rangle - \gamma\mathbb{E}\left\langle\nabla f(\tilde{\boldsymbol{y}}_t) - \nabla f(\tilde{\boldsymbol{x}}_t), \frac{\nabla f(\tilde{\boldsymbol{x}}_t)}{\sqrt{\boldsymbol{v}_t+\epsilon}}\right\rangle
\end{aligned}$$

$$
\begin{aligned}
&-\gamma\mathbb{E}\left\langle \nabla f(\tilde{\boldsymbol{y}}_t)-\nabla f(\tilde{\boldsymbol{x}}_t), \frac{\frac{1}{n}\sum_{i=1}^n \nabla f\left(\boldsymbol{x}_t^{(i)}\right)-\nabla f(\tilde{\boldsymbol{x}}_t)}{\sqrt{\boldsymbol{v}_t+\epsilon}}\right\rangle \\
\leq &-\frac{\gamma\mathbb{E}\left\|\nabla f(\tilde{\boldsymbol{x}}_t)\right\|^2}{\sqrt{G_\infty^2+\epsilon}}+\frac{\gamma\eta_1}{2}\mathbb{E}\left\|\nabla f(\tilde{\boldsymbol{x}}_t)\right\|^2+\frac{\gamma}{2\eta_1}\mathbb{E}\left\|\frac{\frac{1}{n}\sum_{i=1}^n \nabla f\left(\boldsymbol{x}_t^{(i)}\right)-\nabla f(\tilde{\boldsymbol{x}}_t)}{\sqrt{\boldsymbol{v}_t+\epsilon}}\right\|^2+\frac{\gamma\eta_1}{2}\mathbb{E}\left\|\nabla f(\tilde{\boldsymbol{x}}_t)\right\|^2 \\
&+\frac{\gamma}{2\eta_1}\mathbb{E}\left\|\frac{\nabla f(\tilde{\boldsymbol{y}}_t)-\nabla f(\tilde{\boldsymbol{x}}_t)}{\sqrt{\boldsymbol{v}_t+\epsilon}}\right\|^2+\frac{\gamma\eta_1}{2}\mathbb{E}\left\|\nabla f(\tilde{\boldsymbol{y}}_t)-\nabla f(\tilde{\boldsymbol{x}}_t)\right\|^2+\frac{\gamma}{2\eta_1}\mathbb{E}\left\|\frac{\frac{1}{n}\sum_{i=1}^n \nabla f\left(\boldsymbol{x}_t^{(i)}\right)-\nabla f(\tilde{\boldsymbol{x}}_t)}{\sqrt{\boldsymbol{v}_t+\epsilon}}\right\|^2 \\
\leq &-\left(\frac{\gamma}{\sqrt{G_\infty^2+\epsilon}}-\gamma\eta_1\right)\mathbb{E}\left\|\nabla f(\tilde{\boldsymbol{x}}_t)\right\|^2+\frac{\gamma V_1 L^2}{\beta_2^m\eta_1 n}\sum_{i=1}^n\mathbb{E}\left\|\boldsymbol{x}_t^{(i)}-\tilde{\boldsymbol{x}}_t\right\|^2+\left(\frac{\gamma V_1 L^2}{2\beta_2^m\eta_1}+\frac{\gamma\eta_1 L^2}{2}\right)\mathbb{E}\left\|\tilde{\boldsymbol{y}}_t-\tilde{\boldsymbol{x}}_t\right\|^2,
\end{aligned}
$$

where in the last step we use Assumption 1, Lemma 2 and Lemma 4. For the second term, denote the last sync step before t is k, then we have:

$$
\begin{aligned}
\mathbb{E}\left\|\boldsymbol{x}_t^{(i)}-\tilde{\boldsymbol{x}}_t\right\|^2=&\mathbb{E}\left\|\boldsymbol{x}_t^{(i)}-\boldsymbol{x}_k^{(i)}-(\tilde{\boldsymbol{x}}_t-\tilde{\boldsymbol{x}}_k)\right\|^2 \\
\leq&2\mathbb{E}\left\|\boldsymbol{x}_t^{(i)}-\boldsymbol{x}_k^{(i)}\right\|^2+2\mathbb{E}\left\|\tilde{\boldsymbol{x}}_t-\tilde{\boldsymbol{x}}_k\right\|^2 \\
\leq&2\gamma^2\mathbb{E}\left\|\sum_{j=k}^{t-1}\frac{\boldsymbol{m}_j^{(i)}}{\sqrt{\boldsymbol{v}_t+\epsilon}}\right\|^2+2\gamma^2\mathbb{E}\left\|\frac{1}{n}\sum_{i=1}^n\sum_{j=k}^{t-1}\frac{\boldsymbol{m}_j^{(i)}}{\sqrt{\boldsymbol{v}_t+\epsilon}}\right\|^2 \\
\leq&2\gamma^2(t-k)\sum_{j=k}^{t-1}\mathbb{E}\left\|\frac{\boldsymbol{m}_j^{(i)}}{\sqrt{\boldsymbol{v}_t+\epsilon}}\right\|^2+2\gamma^2(t-k)\frac{1}{n}\sum_{i=1}^n\sum_{j=k}^{t-1}\mathbb{E}\left\|\frac{\boldsymbol{m}_j^{(i)}}{\sqrt{\boldsymbol{v}_t+\epsilon}}\right\|^2 \\
\leq&\frac{4\gamma^2H^2V_1M}{\beta_2^m},
\end{aligned}
\tag{3}
$$

where the first step holds because Lemma 4, Lemma 2, and the fact that at the sync step k, $\tilde{\boldsymbol{x}}_k=\boldsymbol{x}_k^{(i)}$. For the third term, we have

$$
\begin{aligned}
\mathbb{E}\left\|\tilde{\boldsymbol{y}}_t-\tilde{\boldsymbol{x}}_t\right\|^2=&\mathbb{E}\left\|\frac{\gamma\tilde{\boldsymbol{m}}_t}{(1-\beta_1)\sqrt{\boldsymbol{v}_t+\epsilon}}+\frac{\gamma\boldsymbol{\delta}_t}{\sqrt{\boldsymbol{v}_t+\epsilon}}\right\|^2 \\
\leq&\frac{2\gamma^2V_1}{\beta_2^m(1-\beta_1)^2}\mathbb{E}\left\|\tilde{\boldsymbol{m}}_t\right\|^2+\frac{2V_1}{\beta_2^m}\mathbb{E}\left\|\gamma\boldsymbol{\delta}_t\right\|^2 \\
\overset{Lemma\ 7}{\leq}&\frac{2\gamma^2V_1M}{\beta_2^m(1-\beta_1)^2}+\frac{2\gamma^2V_1}{\beta_2^m}\cdot4\Delta^2 \\
\leq&\frac{2\gamma^2V_1M}{\beta_2^m(1-\beta_1)^2}+\frac{8\gamma^2V_1\Delta^2}{\beta_2^m},
\end{aligned}
\tag{4}
$$

where we again apply the Lemma 2 and Lemma 4. Then we can get

$$
\begin{aligned}
A_1\leq&-\left(\frac{\gamma}{\sqrt{G_\infty^2+\epsilon}}-\gamma\eta_1\right)\mathbb{E}\left\|\nabla f(\tilde{\boldsymbol{x}}_t)\right\|^2+\frac{\gamma V_1L^2}{\beta_2^m\eta_1 n}\sum_{i=1}^n\mathbb{E}\left\|\boldsymbol{x}_t^{(i)}-\tilde{\boldsymbol{x}}_t\right\|^2+\left(\frac{\gamma V_1L^2}{2\beta_2^m\eta_1}+\frac{\gamma\eta_1L^2}{2}\right)\mathbb{E}\left\|\tilde{\boldsymbol{y}}_t-\tilde{\boldsymbol{x}}_t\right\|^2 \\
\leq&-\left(\frac{\gamma}{\sqrt{G_\infty^2+\epsilon}}-\gamma\eta_1\right)\mathbb{E}\left\|\nabla f(\tilde{\boldsymbol{x}}_t)\right\|^2+\frac{4\gamma^3H^2V_1^2L^2M}{\beta_2^m\eta_1}+\left(\frac{\gamma V_1L^2}{2\beta_2^m\eta_1}+\frac{\gamma\eta_1L^2}{2}\right)\cdot\left(\frac{2\gamma^2V_1M}{\beta_2^m(1-\beta_1)^2}+\frac{8\gamma^2V_1\Delta^2}{\beta_2^m}\right) \\
\leq&-\left(\frac{\gamma}{\sqrt{G_\infty^2+\epsilon}}-\gamma\eta_1\right)\mathbb{E}\left\|\nabla f(\tilde{\boldsymbol{x}}_t)\right\|^2+\frac{4\gamma^3H^2V_1^2L^2M}{\beta_2^m\eta_1}+\frac{\gamma^3V_1^2ML^2}{\eta_1\beta_2^{2m}(1-\beta_1)^2}+\frac{\gamma^3\eta_1V_1ML^2}{\beta_2^m(1-\beta_1)^2}+\frac{4\gamma^3V_1^2\Delta^2L^2}{\eta_1\beta_2^{2m}} \\
&+\frac{4\gamma^3\eta_1V_1\Delta^2L^2}{\beta_2^m}.
\end{aligned}
$$

where in the second step we reuse Equation (3). Next we can bound A_2 as follows

$$\begin{aligned}
A_2 =& L\gamma^2\mathbb{E}\left\|\frac{\tilde{\boldsymbol{g}}_t}{\sqrt{\boldsymbol{v}_t+\epsilon}}\right\|^2 \\
\leq& \frac{L\gamma^2 V_1}{\beta_2^m}\mathbb{E}\left\|\frac{1}{n}\sum_{i=1}^n \boldsymbol{g}_t^{(i)}\right\|^2 \\
\leq& \frac{L\gamma^2 V_1\sigma^2}{n\beta_2^m} + \frac{L\gamma^2 V_1}{\beta_2^m}\mathbb{E}\left\|\frac{1}{n}\sum_{i=1}^n \nabla f\left(\boldsymbol{x}_t^{(i)}\right)\right\|^2 \\
\leq& \frac{L\gamma^2 V_1\sigma^2}{n\beta_2^m} + \frac{2L\gamma^2 V_1}{\beta_2^m}\mathbb{E}\left\|\frac{1}{n}\sum_{i=1}^n \nabla f\left(\boldsymbol{x}_t^{(i)}\right) - \nabla f(\tilde{\boldsymbol{x}}_t)\right\|^2 + \frac{2L\gamma^2 V_1}{\beta_2^m}\mathbb{E}\left\|\nabla f(\tilde{\boldsymbol{x}}_t)\right\|^2 \\
\leq& \frac{L\gamma^2 V_1\sigma^2}{n\beta_2^m} + \frac{2L\gamma^2 V_1 L^2}{n\beta_2^m}\sum_{i=1}^n \mathbb{E}\left\|\boldsymbol{x}_t^{(i)} - \tilde{\boldsymbol{x}}_t\right\|^2 + \frac{2L\gamma^2 V_1}{\beta_2^m}\mathbb{E}\left\|\nabla f(\tilde{\boldsymbol{x}}_t)\right\|^2 \\
\leq& \frac{L\gamma^2 V_1\sigma^2}{n\beta_2^m} + \frac{8\gamma^3 V_1^2 H^2 M L^3}{\beta_2^m} + \frac{2L\gamma^2 V_1}{\beta_2^m}\mathbb{E}\left\|\nabla f(\tilde{\boldsymbol{x}}_t)\right\|^2,
\end{aligned}$$

where in the sixth step we reuse Equation (3). For A_3,

$$\begin{aligned}
A_3 =& -\gamma\mathbb{E}\left\langle\nabla f(\tilde{\boldsymbol{y}}_t), \boldsymbol{q}_t\right\rangle \\
=& -\gamma\mathbb{E}\left\langle\nabla f(\tilde{\boldsymbol{x}}_t), \boldsymbol{q}_t\right\rangle - \gamma\mathbb{E}\left\langle\nabla f(\tilde{\boldsymbol{y}}_t) - \nabla f(\tilde{\boldsymbol{x}}_t), \boldsymbol{q}_t\right\rangle \\
\overset{\forall\eta_2>0}{\leq}& \frac{\gamma\eta_2}{2}\mathbb{E}\left\|\nabla f(\tilde{\boldsymbol{x}}_t)\right\|^2 + \frac{\gamma\eta_2}{2}\mathbb{E}\left\|\nabla f(\tilde{\boldsymbol{y}}_t) - \nabla f(\tilde{\boldsymbol{x}}_t)\right\|^2 + \frac{\gamma}{\eta_2}\mathbb{E}\left\|\boldsymbol{q}_t\right\|^2 \\
\leq& \frac{\gamma\eta_2}{2}\mathbb{E}\left\|\nabla f(\tilde{\boldsymbol{x}}_t)\right\|^2 + \frac{\gamma\eta_2 L^2}{2}\cdot\left(\frac{2\gamma^2 V_1 M}{\beta_2^m(1-\beta_1)^2} + \frac{8\gamma^2 V_1\Delta^2}{\beta_2^m}\right) + \frac{\gamma}{\eta_2}\mathbb{E}\left\|\boldsymbol{q}_t\right\|^2 \\
\leq& \frac{\gamma\eta_2}{2}\mathbb{E}\left\|\nabla f(\tilde{\boldsymbol{x}}_t)\right\|^2 + \frac{\gamma^3\eta_2 V_1 M L^2}{\beta_2^m(1-\beta_1)^2} + \frac{4\gamma^3\eta_2 V_1\Delta^2 L^2}{\beta_2^m} + \frac{\gamma}{\eta_2}\mathbb{E}\left\|\boldsymbol{q}_t\right\|^2,
\end{aligned}$$

where in the last step we reuse Equation (4). Combine the bound of A_1 to A_4, we obtain

$$\begin{aligned}
&\mathbb{E}f(\tilde{\boldsymbol{y}}_{t+1}) - \mathbb{E}f(\tilde{\boldsymbol{y}}_t) \\
\leq& -\left(\frac{\gamma}{\sqrt{G_\infty^2+\epsilon}} - \gamma\eta_1 - \frac{\gamma\eta_2}{2}\right)\mathbb{E}\left\|\nabla f(\tilde{\boldsymbol{x}}_t)\right\|^2 + \frac{4\gamma^3 H^2 V_1^2 L^2 M}{\beta_2^m\eta_1} + \frac{\gamma^3 V_1^2 M L^2}{\eta_1\beta_2^{2m}(1-\beta_1)^2} + \frac{\gamma^3\eta_1 V_1 M L^2}{\beta_2^m(1-\beta_1)^2} + \frac{4\gamma^3 V_1^2\Delta^2 L^2}{\eta_1\beta_2^{2m}} \\
&+ \frac{4\gamma^3\eta_1 V_1\Delta^2 L^2}{\beta_2^m} + \frac{L\gamma^2 V_1\sigma^2}{n\beta_2^m} + \frac{8\gamma^3 V_1^2 H^2 M L^3}{\beta_2^m} + \frac{2L\gamma^2 V_1}{\beta_2^m}\mathbb{E}\left\|\nabla f(\tilde{\boldsymbol{x}}_t)\right\|^2 + \frac{\gamma^3\eta_2 V_1 M L^2}{\beta_2^m(1-\beta_1)^2} + \frac{4\gamma^3\eta_2 V_1\Delta^2 L^2}{\beta_2^m} \\
&+ \left(\frac{\gamma}{\eta_2} + L\gamma^2\right)\mathbb{E}\left\|\boldsymbol{q}_t\right\|^2.
\end{aligned}$$

We set the two constants η_1, η_2 as

$$\begin{aligned}
\eta_1 =& \frac{1}{4\sqrt{G_\infty^2+\epsilon}} \\
\eta_2 =& \frac{1}{2\sqrt{G_\infty^2+\epsilon}},
\end{aligned}$$

then we have,

$$\begin{aligned}
&\mathbb{E}f(\tilde{\boldsymbol{y}}_{t+1}) - \mathbb{E}f(\tilde{\boldsymbol{y}}_t) \\
\leq& -\left(\frac{\gamma}{\sqrt{G_\infty^2+\epsilon}} - \gamma\eta_1 - \frac{\gamma\eta_2}{2}\right)\mathbb{E}\left\|\nabla f(\tilde{\boldsymbol{x}}_t)\right\|^2 + \frac{4\gamma^3 H^2 V_1^2 L^2 M}{\beta_2^m\eta_1} + \frac{\gamma^3 V_1^2 M L^2}{\eta_1\beta_2^{2m}(1-\beta_1)^2} + \frac{\gamma^3\eta_1 V_1 M L^2}{\beta_2^m(1-\beta_1)^2} + \frac{4\gamma^3 V_1^2\Delta^2 L^2}{\eta_1\beta_2^{2m}}
\end{aligned}$$

$$
\begin{aligned}
&+\frac{4\gamma^3\eta_1 V_1\Delta^2L^2}{\beta_2^m}+\frac{L\gamma^2V_1\sigma^2}{n\beta_2^m}+\frac{8\gamma^3V_1^2H^2ML^3}{\beta_2^m}+\frac{2L\gamma^2V_1}{\beta_2^m}\mathbb{E}\left\|\nabla f(\tilde{\boldsymbol{x}}_t)\right\|^2+\frac{\gamma^3\eta_2V_1ML^2}{\beta_2^m(1-\beta_1)^2}+\frac{4\gamma^3\eta_2V_1\Delta^2L^2}{\beta_2^m}\\
&+\left(\frac{\gamma}{\eta_2}+L\gamma^2\right)\mathbb{E}\left\|\boldsymbol{q}_t\right\|^2\\
\leq&-\left(\frac{\gamma}{2\sqrt{G_\infty^2+\epsilon}}-\frac{2L\gamma^2V_1}{\beta_2^m}\right)\mathbb{E}\left\|\nabla f(\tilde{\boldsymbol{x}}_t)\right\|^2+\frac{36\gamma^3H^2V_1(M+\Delta^2)L^2(1+L)(G_\infty^2+\epsilon+1)}{\beta_2^m(1-\beta_1)^2\sqrt{G_\infty^2+\epsilon}}\\
&+\frac{L\gamma^2V_1\sigma^2}{n\beta_2^m}+\left(2\gamma\sqrt{G_\infty^2+\epsilon}+L\gamma^2\right)\mathbb{E}\left\|\boldsymbol{q}_t\right\|^2.
\end{aligned}
$$

Finally, we need to bound the norm of $\boldsymbol{q}_t$. If we denote the last sync step was k steps before t, then,

$$
\begin{aligned}
\boldsymbol{q}_t=&\tilde{\boldsymbol{x}}_{t+1}-\tilde{\boldsymbol{x}}_{t+\frac{1}{2}}-\frac{\gamma}{(1-\beta_1)\sqrt{\boldsymbol{v}_t+\epsilon}}\left(\tilde{\boldsymbol{m}}_{t+1}-\tilde{\boldsymbol{m}}_{t+\frac{1}{2}}\right)-\frac{\gamma\boldsymbol{\delta}_{t+1}-\gamma\boldsymbol{\delta}_t}{\sqrt{\boldsymbol{v}_t+\epsilon}}\\
=&\tilde{\boldsymbol{x}}_{t+1}-\tilde{\boldsymbol{x}}_{t-k+1}+\tilde{\boldsymbol{x}}_{t-k+1}-\tilde{\boldsymbol{x}}_{t+\frac{1}{2}}-\frac{\gamma}{(1-\beta_1)\sqrt{\boldsymbol{v}_t+\epsilon}}\left(\tilde{\boldsymbol{m}}_{t+1}-\tilde{\boldsymbol{m}}_{t+\frac{1}{2}}\right)-\frac{\gamma\boldsymbol{\delta}_{t+1}-\gamma\boldsymbol{\delta}_t}{\sqrt{\boldsymbol{v}_t+\epsilon}}\\
=&-\frac{\gamma\tilde{\boldsymbol{u}}_{t+\frac{1}{2}}}{\sqrt{\boldsymbol{v}_t+\epsilon}}-\left(\sum_{j=t-k+1}^{t}\frac{\gamma\tilde{\boldsymbol{m}}_j}{\sqrt{\boldsymbol{v}_t+\epsilon}}\right)-\frac{\gamma\left(\tilde{\boldsymbol{m}}_{t+1}-\tilde{\boldsymbol{m}}_{t+\frac{1}{2}}\right)}{(1-\beta_1)\sqrt{\boldsymbol{v}_t+\epsilon}}\\
=&-\frac{\gamma}{(1-\beta_1)\sqrt{\boldsymbol{v}_t+\epsilon}}\left(\tilde{\boldsymbol{m}}_{t+1}-\tilde{\boldsymbol{m}}_{t+\frac{1}{2}}+2(1-\beta_1)\sum_{j=t-k+1}^{t}\tilde{\boldsymbol{m}}_j\right),
\end{aligned}
$$

based on which we obtain

$$
\begin{aligned}
\mathbb{E}\left\|\boldsymbol{q}_t\right\|^2=&\mathbb{E}\left\|\frac{\gamma}{(1-\beta_1)\sqrt{\boldsymbol{v}_t+\epsilon}}\left(\tilde{\boldsymbol{m}}_{t+1}-\tilde{\boldsymbol{m}}_{t+\frac{1}{2}}+2(1-\beta_1)\sum_{j=t-k+1}^{t}\tilde{\boldsymbol{m}}_j\right)\right\|^2\\
\leq&\frac{\gamma^2V_1}{\beta_2^m(1-\beta_1)^2}\left(3\mathbb{E}\left\|\tilde{\boldsymbol{m}}_{t+1}\right\|^2+3\mathbb{E}\left\|\tilde{\boldsymbol{m}}_{t+\frac{1}{2}}\right\|^2+12(1-\beta_1)^2k\sum_{j=t-k+1}^{t}\mathbb{E}\left\|\tilde{\boldsymbol{m}}_j\right\|^2\right)\\
\leq&\frac{12\gamma^2V_1(H+1)^2M}{\beta_2^m(1-\beta_1)^2}.
\end{aligned}
$$

Put everything together, and let γ fulfills

$$
\gamma\leq\min\left\{\frac{\beta_2^m}{4V_1L\sqrt{G_\infty^2+\epsilon}},\frac{2\sqrt{G_\infty^2+\epsilon}}{L}\right\},
$$

we finally obtain

$$
\begin{aligned}
&\mathbb{E}f(\tilde{\boldsymbol{y}}_{t+1})-\mathbb{E}f(\tilde{\boldsymbol{y}}_t)\\
\leq&-\frac{\gamma\mathbb{E}\left\|\nabla f(\tilde{\boldsymbol{x}}_t)\right\|^2}{4\sqrt{G_\infty^2+\epsilon}}+\frac{36\gamma^3H^2V_1(M+\Delta^2)L^2(1+L)(G_\infty^2+\epsilon+1)}{\beta_2^m(1-\beta_1)^2\sqrt{G_\infty^2+\epsilon}}+\frac{L\gamma^2V_1\sigma^2}{n\beta_2^m}+\frac{48\gamma^3V_1(H+1)^2M\sqrt{G_\infty^2+\epsilon}}{\beta_2^m(1-\beta_1)^2}.
\end{aligned}
$$

To this end, we have provided bound to all the sync steps t with ($t\notin\mathcal{T}_{\boldsymbol{v}}$ and $t\in\mathcal{T}_{\boldsymbol{u}}$). For all the t with ($t\notin\mathcal{T}_{\boldsymbol{v}}$ and $t\notin\mathcal{T}_{\boldsymbol{u}}$), they can be seen as a special case of $\boldsymbol{q}_t=\boldsymbol{0}$. Since $A_3+A_4>0$, this bound will continue to hold for them, so that to sum over all the t with $t\notin\mathcal{T}_{\boldsymbol{v}}$, we obtain

$$
\begin{aligned}
&\sum_{t\notin\mathcal{T}_{\boldsymbol{v}}}\frac{\gamma\mathbb{E}\left\|\nabla f(\tilde{\boldsymbol{x}}_t)\right\|^2}{4\sqrt{G_\infty^2+\epsilon}}\\
\leq&\sum_{t\notin\mathcal{T}_{\boldsymbol{v}}}\mathbb{E}f(\tilde{\boldsymbol{y}}_t)-\mathbb{E}f(\tilde{\boldsymbol{y}}_{t+1})+\frac{36\gamma^3H^2V_1(3G_\infty^2d+25\Delta^2)L^2(1+L)(G_\infty^2+\epsilon+1)(T-m)}{\beta_2^m(1-\beta_1)^4\sqrt{G_\infty^2+\epsilon}}+\frac{L\gamma^2V_1\sigma^2(T-m)}{n\beta_2^m}
\end{aligned}
$$

$$+\frac{48\gamma^3 V_1(H+1)^2(3G_\infty^2 d+24\Delta^2)\sqrt{G_\infty^2+\epsilon}(T-m)}{\beta_2^m(1-\beta_1)^4},$$

where we replace M with Lemma 8. That completes the proof. □

Lemma 10. *In Algorithm 2, For all the $t \geq 0$ that fulfills $\boldsymbol{v}_t \neq \boldsymbol{v}_{t+1}$, i.e. $t \in \mathcal{T}_{\boldsymbol{v}}$, if the learning rate fulfills*

$$\gamma < \frac{1}{6}$$

, the following bound holds

$$\sum_{t\in\mathcal{T}_{\boldsymbol{v}}}\frac{\gamma\mathbb{E}\|\nabla f(\tilde{\boldsymbol{x}}_t)\|^2}{4\sqrt{G_\infty^2+\epsilon}} \leq \sum_{t\in\mathcal{T}_{\boldsymbol{v}}}\mathbb{E}f(\tilde{\boldsymbol{y}}_t)-\mathbb{E}f(\tilde{\boldsymbol{y}}_{t+1})+\frac{2\gamma\sigma^2 m}{nL}+\frac{106\gamma H^2 V_1(M+\Delta^2)mL}{\beta_2^m(1-\beta_1)^2}+\frac{\gamma\sigma^2 m}{4n\sqrt{G_\infty^2+\epsilon}}+\frac{\gamma G_\infty^2 dm}{4\sqrt{G_\infty^2+\epsilon}}.$$

Proof. From the definition of the auxiliary sequence, we obtain,

$$\tilde{\boldsymbol{y}}_{t+1}-\tilde{\boldsymbol{y}}_t=\tilde{\boldsymbol{x}}_{t+1}-\tilde{\boldsymbol{x}}_t-\frac{\gamma}{1-\beta_1}\left(\frac{\tilde{\boldsymbol{m}}_{t+1}}{\sqrt{\boldsymbol{v}_{t+1}+\epsilon}}-\frac{\tilde{\boldsymbol{m}}_t}{\sqrt{\boldsymbol{v}_t+\epsilon}}\right)-\left(\frac{\gamma\boldsymbol{\delta}_{t+1}}{\sqrt{\boldsymbol{v}_{t+1}+\epsilon}}-\frac{\gamma\boldsymbol{\delta}_t}{\sqrt{\boldsymbol{v}_t+\epsilon}}\right).$$

Based on Assumption 1,

$$\begin{aligned}
&\mathbb{E}f(\tilde{\boldsymbol{y}}_{t+1})-\mathbb{E}f(\tilde{\boldsymbol{y}}_t)\\
\leq&\mathbb{E}\left\langle\nabla f(\tilde{\boldsymbol{y}}_t),\tilde{\boldsymbol{y}}_{t+1}-\tilde{\boldsymbol{y}}_t\right\rangle+\frac{L}{2}\mathbb{E}\left\|\tilde{\boldsymbol{y}}_{t+1}-\tilde{\boldsymbol{y}}_t\right\|^2\\
\overset{\gamma\eta<1}{\leq}&\frac{\eta\gamma}{2L}\mathbb{E}\left\|\nabla f(\tilde{\boldsymbol{y}}_t)\right\|^2+\frac{L}{\eta\gamma}\mathbb{E}\left\|\tilde{\boldsymbol{y}}_{t+1}-\tilde{\boldsymbol{y}}_t\right\|^2\\
\leq&\frac{\eta\gamma}{L}\mathbb{E}\left\|\nabla f(\tilde{\boldsymbol{x}}_t)\right\|^2+\eta\gamma L\mathbb{E}\left\|\tilde{\boldsymbol{y}}_t-\tilde{\boldsymbol{x}}_t\right\|^2+\frac{L}{\eta\gamma}\mathbb{E}\left\|\tilde{\boldsymbol{y}}_{t+1}-\tilde{\boldsymbol{y}}_t\right\|^2\\
\leq&\frac{2\eta\gamma}{L}\mathbb{E}\left\|\nabla f(\tilde{\boldsymbol{x}}_t)-\frac{1}{n}\sum_{i=1}^n\nabla f\left(\boldsymbol{x}_t^{(i)}\right)\right\|^2+\frac{2\eta\gamma}{L}\mathbb{E}\left\|\frac{1}{n}\sum_{i=1}^n\nabla f\left(\boldsymbol{x}_t^{(i)}\right)-\frac{1}{n}\sum_{i=1}^n\boldsymbol{g}_t^{(i)}\right\|^2+\eta\gamma L\mathbb{E}\left\|\tilde{\boldsymbol{y}}_t-\tilde{\boldsymbol{x}}_t\right\|^2\\
&+\frac{L}{\eta\gamma}\mathbb{E}\left\|\tilde{\boldsymbol{y}}_{t+1}-\tilde{\boldsymbol{y}}_t\right\|^2\\
\leq&\frac{2\eta\gamma L}{n}\sum_{i=1}^n\mathbb{E}\left\|\tilde{\boldsymbol{x}}_t-\boldsymbol{x}_t^{(i)}\right\|^2+\frac{2\eta\gamma\sigma^2}{nL}+\eta\gamma L\mathbb{E}\left\|\tilde{\boldsymbol{y}}_t-\tilde{\boldsymbol{x}}_t\right\|^2+\frac{L}{\eta\gamma}\mathbb{E}\left\|\tilde{\boldsymbol{y}}_{t+1}-\tilde{\boldsymbol{y}}_t\right\|^2.
\end{aligned}$$

We now bound the three norm terms separately. From Equation (3), we obtain for the first term,

$$\mathbb{E}\left\|\boldsymbol{x}_t^{(i)}-\tilde{\boldsymbol{x}}_t\right\|^2\leq\frac{4\gamma^2H^2V_1M}{\beta_2^m},$$

where we again use M to denote the constant bound from Lemma 8 for brevity. On the other hand, based on a similar derivation to Equation (4), we obtain

$$\mathbb{E}\left\|\tilde{\boldsymbol{y}}_t-\tilde{\boldsymbol{x}}_t\right\|^2\leq\frac{2\gamma^2V_1M}{\beta_2^m(1-\beta_1)^2}+\frac{8\gamma^2V_1\Delta^2}{\beta_2^m}.$$

Finally, for the last norm, it's possible that the update towards $t+1$ step contains synchronization on the buffer. So that we need to discuss the two cases separately. First, for all the $t\in\mathcal{T}_{\boldsymbol{u}}$, denote the last sync step before t is k, then we have

$$\begin{aligned}
&\mathbb{E}\left\|\tilde{\boldsymbol{y}}_{t+1}-\tilde{\boldsymbol{y}}_t\right\|^2\\
=&\mathbb{E}\left\|\tilde{\boldsymbol{x}}_{t+1}-\tilde{\boldsymbol{x}}_t-\frac{\gamma}{1-\beta_1}\left(\frac{\tilde{\boldsymbol{m}}_{t+1}}{\sqrt{\boldsymbol{v}_{t+1}+\epsilon}}-\frac{\tilde{\boldsymbol{m}}_t}{\sqrt{\boldsymbol{v}_t+\epsilon}}\right)-\left(\frac{\gamma\boldsymbol{\delta}_{t+1}}{\sqrt{\boldsymbol{v}_{t+1}+\epsilon}}-\frac{\gamma\boldsymbol{\delta}_t}{\sqrt{\boldsymbol{v}_t+\epsilon}}\right)\right\|^2\\
\leq&7\mathbb{E}\left\|\tilde{\boldsymbol{x}}_{t+1}-\tilde{\boldsymbol{x}}_{t-k+1}\right\|^2+7\mathbb{E}\left\|\tilde{\boldsymbol{x}}_{t-k+1}-\tilde{\boldsymbol{x}}_{t+\frac{1}{2}}\right\|^2+7\mathbb{E}\left\|\tilde{\boldsymbol{x}}_{t+\frac{1}{2}}-\tilde{\boldsymbol{x}}_t\right\|^2+\frac{7\gamma^2}{1-\beta_1}\mathbb{E}\left\|\frac{\tilde{\boldsymbol{m}}_{t+1}}{\sqrt{\boldsymbol{v}_{t+1}+\epsilon}}\right\|^2
\end{aligned}$$

$$
\begin{aligned}
&+\frac{7\gamma^2}{1-\beta_1}\mathbb{E}\left\|\frac{\tilde{\boldsymbol{m}}_t}{\sqrt{\boldsymbol{v}_t+\epsilon}}\right\|^2+7\mathbb{E}\left\|\frac{\gamma\boldsymbol{\delta}_{t+1}}{\sqrt{\boldsymbol{v}_{t+1}+\epsilon}}\right\|^2+7\mathbb{E}\left\|\frac{\gamma\boldsymbol{\delta}_t}{\sqrt{\boldsymbol{v}_t+\epsilon}}\right\|^2\\
\leq&7\mathbb{E}\left\|\tilde{\boldsymbol{x}}_{t+1}-\tilde{\boldsymbol{x}}_{t-k+1}\right\|^2+7\mathbb{E}\left\|\tilde{\boldsymbol{x}}_{t-k+1}-\tilde{\boldsymbol{x}}_{t+\frac{1}{2}}\right\|^2+7\gamma^2\mathbb{E}\left\|\frac{\tilde{\boldsymbol{m}}_t}{\sqrt{\boldsymbol{v}_t+\epsilon}}\right\|^2+\frac{7\gamma^2}{1-\beta_1}\mathbb{E}\left\|\frac{\tilde{\boldsymbol{m}}_{t+1}}{\sqrt{\boldsymbol{v}_{t+1}+\epsilon}}\right\|^2\\
&+\frac{7\gamma^2}{1-\beta_1}\mathbb{E}\left\|\frac{\tilde{\boldsymbol{m}}_t}{\sqrt{\boldsymbol{v}_t+\epsilon}}\right\|^2+7\mathbb{E}\left\|\frac{\gamma\boldsymbol{\delta}_{t+1}}{\sqrt{\boldsymbol{v}_{t+1}+\epsilon}}\right\|^2+7\mathbb{E}\left\|\frac{\gamma\boldsymbol{\delta}_t}{\sqrt{\boldsymbol{v}_t+\epsilon}}\right\|^2\\
\leq&7\mathbb{E}\left\|\frac{\sum_{j=t-k+1}^t\gamma\tilde{\boldsymbol{m}}_j+\boldsymbol{\delta}_t-\boldsymbol{\delta}_{t+1}}{\sqrt{\boldsymbol{v}_k+\epsilon}}\right\|^2+7\mathbb{E}\left\|\frac{\sum_{j=t-k+1}^t\gamma\tilde{\boldsymbol{m}}_j}{\sqrt{\boldsymbol{v}_k+\epsilon}}\right\|^2+7\gamma^2\mathbb{E}\left\|\frac{\tilde{\boldsymbol{m}}_t}{\sqrt{\boldsymbol{v}_t+\epsilon}}\right\|^2+\frac{7\gamma^2}{1-\beta_1}\mathbb{E}\left\|\frac{\tilde{\boldsymbol{m}}_{t+1}}{\sqrt{\boldsymbol{v}_{t+1}+\epsilon}}\right\|^2\\
&+\frac{7\gamma^2}{1-\beta_1}\mathbb{E}\left\|\frac{\tilde{\boldsymbol{m}}_t}{\sqrt{\boldsymbol{v}_t+\epsilon}}\right\|^2+7\mathbb{E}\left\|\frac{\gamma\boldsymbol{\delta}_{t+1}}{\sqrt{\boldsymbol{v}_{t+1}+\epsilon}}\right\|^2+7\mathbb{E}\left\|\frac{\gamma\boldsymbol{\delta}_t}{\sqrt{\boldsymbol{v}_t+\epsilon}}\right\|^2\\
\leq&\frac{105\gamma^2H^2V_1(M+\Delta^2)}{\beta_2^m(1-\beta_1)^2},
\end{aligned}
$$

where in the last step we use Lemma 7, 8 and 4. It is straightforward to verify that this bound also holds for $t\notin\mathcal{T}_{\boldsymbol{u}}$ (since there will be no noise from the sync step). Combine the three norm term bounds, we obtain

$$
\begin{aligned}
&\mathbb{E}f(\tilde{\boldsymbol{y}}_{t+1})-\mathbb{E}f(\tilde{\boldsymbol{y}}_t)\\
\leq&\frac{2\eta\gamma L}{n}\sum_{i=1}^n\mathbb{E}\left\|\tilde{\boldsymbol{x}}_t-\boldsymbol{x}_t^{(i)}\right\|^2+\frac{2\eta\gamma\sigma^2}{nL}+\eta\gamma L\mathbb{E}\left\|\tilde{\boldsymbol{y}}_t-\tilde{\boldsymbol{x}}_t\right\|^2+\frac{L}{\eta\gamma}\mathbb{E}\left\|\tilde{\boldsymbol{y}}_{t+1}-\tilde{\boldsymbol{y}}_t\right\|^2\\
=&\frac{8\eta\gamma^3H^2V_1ML}{\beta_2^m}+\frac{2\eta\gamma\sigma^2}{nL}+\eta\gamma L\left(\frac{2\gamma^2V_1M}{\beta_2^m(1-\beta_1)^2}+\frac{8\gamma^2V_1\Delta^2}{\beta_2^m}\right)+\frac{105\gamma H^2V_1(M+\Delta^2)L}{\eta\beta_2^m(1-\beta_1)^2}\\
\leq&\frac{2\eta\gamma\sigma^2}{nL}+\frac{18\eta\gamma^3H^2V_1ML}{\beta_2^m(1-\beta_1)^2}+\frac{105\gamma H^2V_1(M+\Delta^2)L}{\eta\beta_2^m(1-\beta_1)^2}\\
\leq&\frac{2\gamma\sigma^2}{nL}+\frac{106\gamma H^2V_1(M+\Delta^2)L}{\beta_2^m(1-\beta_1)^2},
\end{aligned}
$$

where in the last step we set $\eta=1$ and use the requirement that $\gamma<1/6$. Summing over all the $t\in\mathcal{T}_{\boldsymbol{v}}$, we get

$$
0\leq\sum_{t\in\mathcal{T}_{\boldsymbol{v}}}\mathbb{E}f(\tilde{\boldsymbol{y}}_t)-\mathbb{E}f(\tilde{\boldsymbol{y}}_{t+1})+\frac{2\gamma\sigma^2m}{nL}+\frac{106\gamma H^2V_1(M+\Delta^2)mL}{\beta_2^m(1-\beta_1)^2}.
$$

Adding $\frac{\gamma}{4\sqrt{G_\infty^2+\epsilon}}\sum_{t\in\mathcal{T}_{\boldsymbol{v}}}\mathbb{E}\|\nabla f(\tilde{\boldsymbol{x}}_t)\|^2$ on both sides, and note that

$$
\begin{aligned}
\sum_{t\in\mathcal{T}_{\boldsymbol{v}}}\mathbb{E}\|\nabla f(\tilde{\boldsymbol{x}}_t)\|^2=&\sum_{t\in\mathcal{T}_{\boldsymbol{v}}}\mathbb{E}\left\|\nabla f(\tilde{\boldsymbol{x}}_t)-\tilde{\boldsymbol{g}}_t\right\|^2+\sum_{t\in\mathcal{T}_{\boldsymbol{v}}}\mathbb{E}\left\|\tilde{\boldsymbol{g}}_t\right\|^2\\
\leq&\frac{\sigma^2m}{n}+G_\infty^2dm.
\end{aligned}
$$

We finally obtain

$$
\sum_{t\in\mathcal{T}_{\boldsymbol{v}}}\frac{\gamma\mathbb{E}\|\nabla f(\tilde{\boldsymbol{x}}_t)\|^2}{4\sqrt{G_\infty^2+\epsilon}}\leq\sum_{t\in\mathcal{T}_{\boldsymbol{v}}}\mathbb{E}f(\tilde{\boldsymbol{y}}_t)-\mathbb{E}f(\tilde{\boldsymbol{y}}_{t+1})+\frac{2\gamma\sigma^2m}{nL}+\frac{106\gamma H^2V_1(M+\Delta^2)mL}{\beta_2^m(1-\beta_1)^2}+\frac{\gamma\sigma^2m}{4n\sqrt{G_\infty^2+\epsilon}}+\frac{\gamma G_\infty^2dm}{4\sqrt{G_\infty^2+\epsilon}}.
$$

That completes the proof. □